

## **Monday Posters**

# Measuring the Acceleration of Free Fall with an Atom Chip BEC Interferometer

F. Baumgärtner<sup>1</sup>, R.J. Sewell<sup>1,2</sup>, I. Llorente-Garcia<sup>1</sup>, J.P. Cotter<sup>1</sup>, J. Dingjan<sup>1</sup>,  
S. Eriksson<sup>1,3</sup>, E.A. Hinds<sup>1</sup>

<sup>1</sup>*Imperial College London, London, United Kingdom*

<sup>2</sup>*Institute of Photonic Sciences, Barcelona, Spain*

<sup>3</sup>*Swansea University, Swansea, Wales, United Kingdom*

We show that a Bose-Einstein condensate (BEC) interferometer on an atom chip<sup>1</sup> is capable of making an absolute force measurement. We demonstrate this by making an absolute measurement of the gravitational acceleration  $g$ .

We implement two interferometer arms by splitting a BEC into two symmetric wells using radio-frequency (rf) adiabatic potentials<sup>2</sup>. The independent control of the rf currents running through the chip surface allows us to change the polarization of the rf field and hence the orientation of the double well potential. Tilting of the system with respect to the horizontal introduces an energy difference  $\Delta E$  and the relative phase between the BECs starts to evolve. After moving the atoms back to their initial position and overlapping the clouds in free fall we measure the resulting phase from the interference pattern. In order to derive a number for  $g$  from experimental results a detailed analysis and understanding of the interferometer scheme is essential. For this type of interferometer we have identified two main limitations to the accuracy of the measurement: a systematic error due to rf field gradients, and a statistical error due to phase spreading from atom-atom interactions. Taking all errors into account we expect a value for  $g$  to within 15%. The statistical uncertainty of the measurement is 5%.

We have a strategy for reducing all systematic errors to less than 1%. In order to reduce the rate of phase spreading we want to squeeze the relative number<sup>3</sup> between the wells in future experiments.

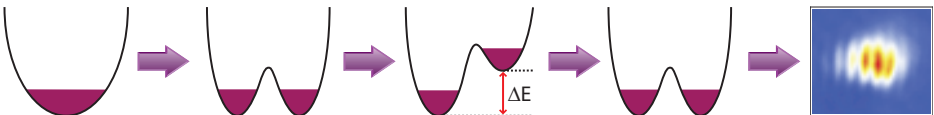


Figure 1: *Experimental scheme of the atom chip BEC interferometer. A single BEC serves as an input state for the interferometer. Tilting of the double well potential introduces an energy difference  $\Delta E$ . The evolution of the relative phase is determined from the resulting interference pattern after recombining the clouds in free fall. The interference pattern shown in the figure is the average of 100 repeated experiments demonstrating phase stability.*

<sup>1</sup>R. J. Sewell et al., J. Phys. B: At. Mol. Opt. Phys. **43**, 051003 (2010)

<sup>2</sup>Schumm et al., Nature Physics **1**, 57 (2005)

<sup>3</sup>G.-B. Jo et al., Phys. Rev. Lett. **98**, 030407 (2007)

# Microwave near-fields on an atom chip: Characterization and use for state-dependent manipulation of ultracold atoms

P. Böhi<sup>1,2</sup>, M.F. Riedel<sup>1,2</sup>, T.W. Hänsch<sup>1,2</sup>, P. Treutlein<sup>1,2,3</sup>

<sup>1</sup>*Fakultät für Physik, Ludwigs-Maximilians-Universität, München, Germany*

<sup>2</sup>*Max-Planck-Institute for Quantum Optics, Garching, Germany*

<sup>3</sup>*Departement Physik, Universität Basel, Basel, Switzerland*

Applications of ultracold neutral atoms in quantum information processing, quantum simulations, and quantum metrology require full coherent control of internal states, motional states, and collisional interactions of the atoms. In quantum information processing, for example, internal states encode the qubits while state-dependent motional dynamics in combination with coherent collisions are used for entanglement generation. To make such entanglement-based technologies a reality, the tools to manipulate the atoms have to be implemented on a simple, robust, and scalable technological platform.

Here, we demonstrate coherent control of internal- and motional state dynamics of atomic Bose-Einstein condensates, using state-dependent microwave near-field potentials which are fully integrated on an atom chip.<sup>1</sup> We reversibly entangle atomic internal and motional states, realizing a trapped-atom interferometer with internal-state labelling. Our system provides control over collisions in mesoscopic condensates, paving the way to on-chip generation of many-particle entanglement and quantum enhanced metrology with spin-squeezed states.<sup>2</sup>

Furthermore, we characterize the microwave near-field using clouds of ultracold atoms which we use as sensitive, tunable and non-invasive probes for microwave field imaging.<sup>3</sup> The microwave magnetic field components drive Rabi oscillations on atomic hyperfine transitions whose frequency can be tuned with a static magnetic field. Readout is accomplished using state-selective absorption imaging. Quantitative data extraction is simple and it is possible to reconstruct the distribution of microwave field amplitudes and phases.

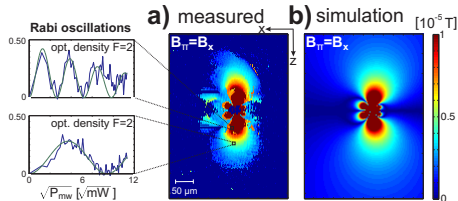


Figure 1: *Comparison of a measured microwave magnetic near-field field polarization component to a simulation. The insets show Rabi oscillations at two exemplary pixels.*

<sup>1</sup>P. Böhi et al., “Coherent manipulation of Bose-Einstein condensates with state-dependent microwave potentials on an atom chip”, *Nat. Phys.* **5**, 592 (2009)

<sup>2</sup>M.F. Riedel et al., “Atom-chip-based generation of entanglement for quantum metrology”, *Nature* **464**, 1170 (2010)

<sup>3</sup>P. Böhi et al., “Imaging of microwave fields using ultracold atoms”, to appear in *Appl. Phys. Lett.*

# Robust Rotational Schrödinger Cats and Heisenberg-Limited Interferometry with Strongly Correlated Ultracold Atoms

Joachim Brand<sup>1</sup> David W. Hallwood<sup>1</sup> Thomas Ernst<sup>1</sup> Jessica J. Cooper<sup>2</sup>

<sup>1</sup>*Centre for Theoretical Chemistry and Physics and Institute of Natural Sciences, Massey University, Private Bag 102904, North Shore, Auckland 0745, New Zealand*

<sup>2</sup>*Quantum Information Science, University of Leeds, United Kingdom*

Large quantum superpositions carry great promise for enhancing precision measurements but can be extremely fragile, currently limiting the size of maximally entangled “NOON” states to 10 particles. The related mesoscopic superpositions of current states with  $10^9$  Cooper pairs observed in superconducting rings have proven more robust but their microscopic nature is debated. Here we present a realistic microscopic model of ultra-cold atoms in a ring trap analogous to superconducting rings. Most importantly, we show how correlations in the strongly-interacting Tonks-Girardeau regime produce superposition states of mesoscopic flow that are robust against single-particle loss and excitation. These states are experimentally accessible and adiabatically connected to NOON states, thus providing a path to engineering larger NOON states. We further show how strongly-correlated superposition states can be used for Heisenberg-limited interferometry of rotational phase shifts. Calculating the Fisher entropy reveals that phase sensitivity degrades less under single-particle loss for these states than it does for NOON states and that the performance is improved compared to classical states.

## Gravimetry with Bose-Einstein Condensates

J.E. Debs, D. Döring, P.A. Altin, G. McDonald, C. Figl, N.P. Robins, J.D. Close

*Australian Centre for Quantum Atom Optics and Department of Quantum Science,  
The Australian National University, Canberra, ACT, Australia*

Gravimetry and gradiometry have become well established tools with applications in areas such as climate monitoring, mineral exploration, and seismology. In recent years, much progress has been made using cold atomic ensembles as sources for atom interferometer based gravimeters and gradiometers. Such sensors are fast becoming viable options as high precision devices for the next generation of application. In general, atomic devices can be more robust, portable, are well controllable, and offer similar or better sensitivities than existing technologies such as falling corner cube sensors<sup>1</sup>. To date, all such sensors have been based on cold *thermal* sources, achieving sensitivities on the order of  $10^{-8}g$  at 1 second of integration<sup>1,2</sup>. One limiting factor in current devices is the temperature of the cloud. For several years our group has worked on developing Bose-condensed sources suitable for atom interferometry<sup>3</sup>, and have become increasingly interested on developing a sensor utilising a Bose-condensed source. We have been building a gravimeter/gradiometer system based on Bose-condensed samples of  $10^6$  Rubidium 87 atoms. We present progress on this device, and preliminary measurements of  $g$ . Building on our previous work developing a projection noise limited atom interferometer<sup>4</sup>, we aim to produce an inertial sensor which utilises squeezed states to enhance the sensitivity of a gravity measurement.

---

<sup>1</sup>A. Peters, K. Y. Chung, and S. Chu, "High-precision gravity measurements using atom interferometry." *Metrologia*, 38, p. 25-61, 2001.

<sup>2</sup>S. Merlet, J. L. Gouet, Q. Bodart, A. Clairon, A. Landragin, F. P. D. Santos, and P. Rouchon, "Operating an atom interferometer beyond its linear range." *Metrologia*, 46 p. 8794, 2009.

<sup>3</sup>J. E. Debs, D. Döring, P. A. Altin, C. Figl, J. Dugué, M. Jeppesen, J. T. Schultz, N. P. Robins, and J. D. Close, "Experimental comparison of raman and rf outcouplers for high-flux atom lasers." *Phys. Rev. A*, 81, 013618, 2010.

<sup>4</sup>D. Döring, G. McDonald, J. E. Debs, C. Figl, P. A. Altin, H.-A. Bachor, N. P. Robins, and J. D. Close, "Quantum-projection-noise-limited interferometry with coherent atoms in a Ramsey-type setup." *Phys. Rev. A*, 81, 043633, Apr 2010.

# Rephasing the nonlinear dynamics of a two-component Bose-Einstein condensate

M. Egorov<sup>1</sup>, R. P. Anderson<sup>1,2</sup>, V. Ivannikov<sup>1,3</sup>, B. V. Hall<sup>1</sup>, A. I. Sidorov<sup>1</sup>

<sup>1</sup>ACQAO and CAOUS, Swinburne University of Technology, Melbourne, Australia

<sup>2</sup>School of Physics, Monash University, Victoria 3800, Australia

<sup>3</sup>Institute of Physics, Saint Petersburg State University, Russia

We observe dephasing and rephasing of a trapped two-component Bose-Einstein condensate macroscopic wavefunction using Ramsey interferometry. This spin-half system is composed of a <sup>87</sup>Rb condensate magnetically trapped on an atom chip and coherently prepared in two hyperfine ground states. Small differences in the inter- and intra-state scattering lengths lead to a spatially inhomogeneous evolution of the relative phase<sup>1</sup> and dephasing which is followed by an increase of the interference contrast when the phase becomes uniform again (self-rephasing). The second type of rephasing is observed after the application of one (Fig. 1a) or up to four spin-echo  $\pi$ -pulses. When coincident with the self-rephasing, the  $\pi$ -pulse of the spin-echo sequence is most efficient. A condensate with 30 000 atoms exhibits several revivals of the Ramsey fringe visibility (Fig. 1b) that occur when the two rephasing mechanisms work in concert. The  $1/e$  decay time of 5 s for successive revival peaks is indicative of long-lived collective spin dynamics. Measurements of the phase randomness for various evolution times with the spin-echo rephasing demonstrate the phase coherence time exceeds 5 s.

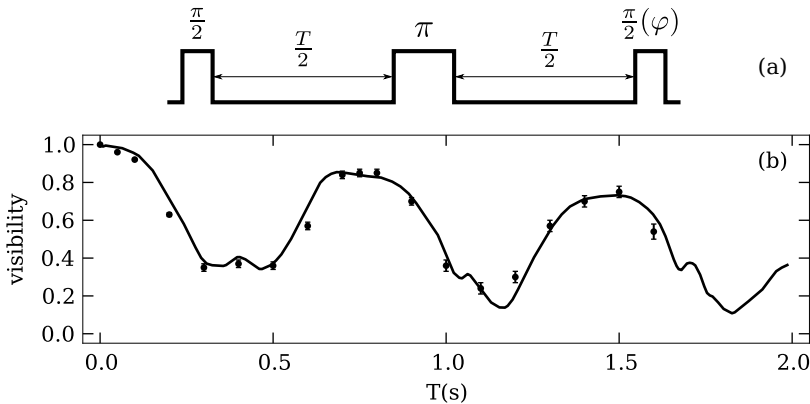


Figure 1: (a) Symmetric echo pulse sequence with variable phase shift ( $\varphi$ ) on the recombining pulse. (b) The visibility of fringes acquired by varying  $\varphi$  depends upon the spatial uniformity of the relative phase. The  $\pi$ -pulse of the echo sequence partially reverses the dynamical spin dephasing, and is most efficient when made coincident with the self-rephasing at  $T = 0.375$  s and 0.75 s. Solid line: mean field theory.

<sup>1</sup>R. P. Anderson, C. Ticknor, A. I. Sidorov and B. V. Hall, *Phys. Rev. A* **80** 023603 (2009).

# Loading an Inductively Coupled Magnetic Ring Trap

P.F. Griffin, A. Dinkelaker, M Vangeleyn, A.S. Arnold, E. Riis

*Department of Physics, SUPA, University of Strathclyde, Glasgow, G4 0NG, UK*

We report on experimental progress towards a ring trap for cold atoms and degenerate quantum gases. A toroidal trapping potential is ideal, not only for storing and investigating atomic systems, but particularly for atom interferometry since the ring provides the guided arms of an interferometer with inherent common mode rejection of many noise sources.

We have previously proposed using an electrically isolated conducting loop in an ac magnetic field to form a toroidal trapping potential<sup>1</sup>. The trapping potential is formed by the superposition of two magnetic fields:

1. an ac, spatially homogenous field produced by external coils,
2. a local field about the loop, created by the induced current.

The two opposite magnetic fields cancel to form a ring of zero magnetic field of varying radius that forms a stable, time-averaged trapping potential. Because there are no electric connections to the conducting loop, the trap can be scaled down to chip size without perturbing the trapping potential.

An <sup>87</sup>Rb magneto-optical trap (MOT) is formed beneath an OFHC copper conducting loop. Following an optical molasses phase the atoms are launched  $\sim 5$  mm vertically in a moving molasses by pulsing on a vertical bias B-field so that the apex of the launch is at the centre of the loop. Atoms may then be trapped by timing the switch-on of the ac, driving B-field. Forced evaporation to degeneracy of bosonic (<sup>87</sup>Rb) and, subsequently, fermionic (<sup>40</sup>K) species can then proceed in the ring geometry by using an additional optical dipole trap to create a hybrid trapping potential.

We will further discuss the application of the ring potential for matter-wave interferometric measurements of inertial and gravitational forces.

---

<sup>1</sup>P.F. Griffin, E. Riis, and A.S. Arnold, "Smooth inductively coupled ring trap for atoms" **77**, 051402(R) (2008)

# Progress on Cold Atom Interferometry Gravimeter

Zhongkun Hu, Minkang Zhou, Xiaochun Duan, Jun Luo

*Department of Physics, Huazhong University of Science and Technology, Wuhan  
430074, P. R. China*

Precisely measuring gravity acceleration  $g$ , a site-dependent quantity that also varies with time, is of great interest for both fundamental research and practical applications, such as the exploration of natural resources and navigation. Instruments used to measure the absolute value of  $g$  have been highly developed during the last decades<sup>1</sup>. The cold atom interferometry gravimeter was firstly used by S.Chu in 1992<sup>2</sup>, sodium atoms were launched and freely falling in an atomic fountain, and the acceleration of sodium atoms was measured by atom interferometry method. For the precision gravity measurement and gravitational experiments, a cold atom gravimeter with resolution  $10^{-9}\text{g/Hz}^{1/2}$  is being built in our lab. This Letter describes the experimental progress of this atomic gravimeter. There are four steps for our Rb87 atom gravimeter: MOT for trapping and launching atoms, the initial state preparation, Raman laser pulse interactions with cold atoms, and the final state detection for interferometry fringes. We have demonstrated a cold atom interferometry gravimeter for gravity measurements, and monitored the local gravity tidal effects.

---

<sup>1</sup>T. Petelski, Atom interferometers for precision gravity measurements, PhD thesis, University of Firenze-University of Paris 6, 2005

<sup>2</sup>A. Peters, K.Y. Chung and S. Chu, High-precision gravity measurements using atom interferometry, Metrologia 38 (2001) 25

# Electromagnetically induced transparency in an erbium-doped crystal

K. Bencheikh<sup>1</sup>, E. Baldit<sup>1</sup>, P. Monnier<sup>1</sup>, J.A. Levenson<sup>1</sup>, S. Briaudeau<sup>2</sup>

<sup>1</sup>*Laboratoire de Photonique et de Nanostructures, Route de Nozay, 91460 Marcoussis, France*

<sup>2</sup>*Institut National de Métrologie, CNAM, 61 rue du Landy, 93210 La Plaine Saint Denis, France*

Electromagnetically Induced Transparency (EIT) has already been demonstrated in different types of solids and has allowed applications such ultraslow light propagation and storage of light pulses. The hyperfine structure of optical transitions in rare-earth ion-doped crystals offers suitable three-level schemes for an efficient implementation of EIT. Oddly enough Erbium doped solid, widely used in communication systems at  $\lambda = 1.5 \mu\text{m}$ , was not investigated until now for EIT applications. In this paper I will report on our investigations conducted in order to 1) determine the hyperfine structure of Erbium-167 ions doped in an  $\text{Y}_2\text{SiO}_5$  crystal, 2) identify  $\Lambda$ -like systems and 3) obtain what we believe is the first observation of EIT using Erbium ions.

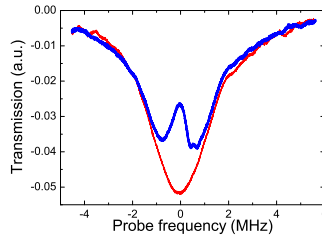


Figure 1: *Transmission of a probe field as the control field is turned on (blue thick line) and off (red thin line).*

The Erbium-167 particular isotope has a nuclear spin  $I = 7/2$  and thus presents a rich hyperfine structure with 16 hyperfine levels in both ground and excited states. Due to the low symmetry of the crystal, all transitions are allowed offering large possibilities for  $\Lambda$ -like systems for EIT. In our investigations, Spectral Hole Burning (SHB) spectroscopy and Electron Paramagnetic Resonance (EPR) spectroscopy are used in order to study the spectroscopic properties of  $^{167}\text{Er}^{3+}:\text{Y}_2\text{SiO}_5$  and to overcome the large inhomogeneous broadening hiding the hyperfine structure. I will first discuss how those spectroscopic techniques have allowed to determine the hyperfine structure of the ground state and to identify two  $\Lambda$ -like schemes suitable for EIT implementation. I will then present the demonstration of EIT (Fig. 1) in both  $\Lambda$ -like systems without any external magnetic field and conclude by discussing the different avenues opened by these demonstrations associated to optical/quantum state preparation.

# Thermal-noise-limited millimeter-size $\text{MgF}_2$ WGM resonator for laser frequency stabilization

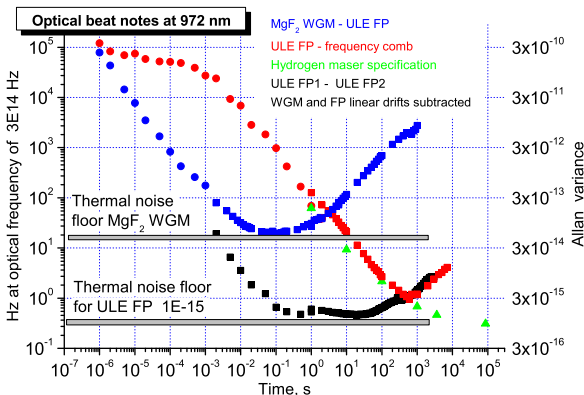
J Alnis<sup>1</sup>, A. Schliesser<sup>1,2</sup>, J. Hofer<sup>1</sup> C. Wang<sup>1,2</sup> T. J. Kippenberg<sup>1,2</sup> T. W. Hänsch<sup>1</sup>

<sup>1</sup>Max Planck Institute of Quantum Optics, Garching D-85748, Germany

<sup>2</sup>Ecole Polytechnique Fdrale de Lausanne, Lausanne CH-1015, Switzerland

Millimeter size whispering gallery mode (WGM) optical resonators made of pure crystalline materials can have optical line width down to a few tens of kHz<sup>1</sup>. This is comparable to high-finesse Fabry Perot (FP) resonators that are important for laser stabilization in precision atomic physics experiments. WGM resonators have several advantages over FP resonators: first, they do not need mirror coatings, thus can be used in very broad wavelength range. In addition, the compact size of WGM resonators allows good temperature stabilization and insensitivity to vibrations.

In this work we report on laser frequency stabilization with a 3 mm diameter WGM  $\text{MgF}_2$  resonator<sup>2</sup> placed in actively stabilized heat shields inside a vacuum chamber. 972 nm light is coupled into the WGM resonator using a prism mounted on a piezo-actuated stage. We compare a WGM-stabilized diode laser to an ULE FP cavity stabilized laser which is an order of magnitude better<sup>3</sup>. Allan plot (see Fig. 1) has a flat floor between 20 ms to 0.5 s which is an indication of thermal noise limit. Thermal noise of this WGM is ca. 40 times bigger compared to ultra-stable ULE FP resonators because of smaller dimensions of WGM. WGM stabilized laser is less noisy than the H maser stabilized optical frequency comb for times between 1E-6 and 3 s. Frequency drift of  $\text{MgF}_2$  resonator is less than 1 kHz/s and typical excursions are within 10 MHz/day, making it suitable for many laser stabilization applications.



<sup>1</sup>A. A. Savchenkov et al., Phys. Rev. A 70, 051804(R) (2004)

<sup>2</sup>J. Hofer, A. Schliesser, and T.J. Kippenberg, arXiv:0911.1178v2

<sup>3</sup>J. Alnis et al., PRA 77, 053809 (2008)

# Laser cooling of atoms in an integrating sphere and its application on cold atom clock

H.D. Cheng<sup>1</sup>, X.C. Wang<sup>2</sup>, Y.L. Meng<sup>2</sup>, B.C. Zheng<sup>2</sup>, L.X. Xiao<sup>1</sup>, L. Liu<sup>1</sup>, Y.Z. Wang<sup>1</sup>

<sup>1</sup>*Key Laboratory for Quantum Optics, Shanghai Institute of Optics and Fine Mechanics, Chinese Academy of Sciences, Shanghai, China*

<sup>2</sup>*Graduate School of the Chinese Academy of Sciences, Beijing, China*

The laser cooling of atoms in an integrating sphere has shown a great potential on building a compact cold atom clock. We have cooled <sup>87</sup>Rb atoms in a ceramic integrating sphere<sup>1</sup>. Cold atoms with number of about 10<sup>8</sup> and temperature of about 25  $\mu$ K were obtained.

Here we will first report an experiment on the measurement of spatial distribution of cooled atoms in the integrating sphere. Since the integrating sphere is nearly closed and thus the conventional imaging method is not applicable, we developed a method to measure the spatial distribution of cold atoms in a closed system. A quadrupole magnetic field is used to shift energy levels of cooled atoms, and a circularized probe beam, which is always resonant with atoms in the zero magnetic field region, is used to detect atoms. The spatial distribution of cold atoms can be mapped by moving the zero point of the quadrupole magnetic field. The results show that the shape of cold atoms is like a dumbbell, which is consistent with the suggestion of Esnault et. al.<sup>2</sup>.

We will also present results on the interaction between microwave and cold atoms in the integrating sphere. The integrating sphere is placed in a cylinder microwave cavity which is resonant at 6.835 GHz on a TE<sub>011</sub> mode. The clock signal is obtained by measuring the population difference before and after the microwave interrogation. The observed Ramsey fringes of the clock transition will be presented.

---

<sup>1</sup>H.D. Cheng, W.Z. Zhang, H.Y. Ma, L. Liu and Y.Z. Wang, "Laser Cooling of rubidium atoms from background vapor in diffuse light.", *Phys. Rev. A* 79, 023407 (2009).

<sup>2</sup>F.X. Esnault, S. Perrin, S. Tremine, S. Guerandel, D. Holleville, N. Dimarcq, V. Hermann and J. Delporte, "Stability of the compact cold atom clock HORACE:", in Proceedings of the 2007 IEEE International Frequency Control Symposium, Joint with the 21st European Frequency and Time Forum (2007).

## **Al<sup>+</sup> Optical Clocks\***

C. W. Chou, D. B. Hume, D. J. Wineland, T. Rosenband

*Time and Frequency Division, National Institute of Standards and Technology, Boulder,  
Colorado 80305, United States of America*

We have constructed an optical clock based on quantum logic spectroscopy of an Al<sup>+</sup> ion that has a fractional frequency inaccuracy of  $8.6 \times 10^{-18}$ . The  $^1S_0 \leftrightarrow ^3P_0$  clock transition resonance has a measured  $Q = 4.2 \times 10^{14}$ . The frequency of a laser stabilized to this transition is compared to that of a previously constructed Al<sup>+</sup> optical clock with a statistical measurement uncertainty of  $7.0 \times 10^{-18}$ . The two clocks exhibit a fractional frequency difference of  $1.8 \times 10^{-17}$ , and a relative stability of  $2.8 \times 10^{-15} \tau^{-1/2}$ . The measured frequency difference is consistent with the accuracy limit of the older clock. We observe small relativistic effects by comparing the frequencies of the clocks. Specifically, time dilation due to velocities less than 10 m/s and gravitational red shift from a 0.33 m height change of one of the clocks lead to measurable differences in the frequencies of the clocks. In addition, we have compared two ion frequency standards with stability unconstrained by laser coherence time.

\*Supported by ONR

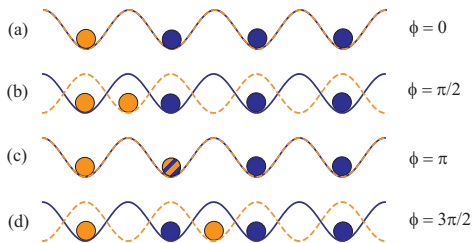
# Entangling the lattice clock: Towards Heisenberg-limited timekeeping

Jonathan D. Weinstein, Kyle Beloy, Andrei Derevianko

*Department of Physics, University of Nevada, Reno, NV 89557, USA*

We present a scheme for entangling thousands of atoms of an optical lattice to reduce the quantum projection noise of a clock measurement. The divalent clock atoms are held in a lattice at a “magic” wavelength that does not perturb the clock frequency, while an open-shell  $J = 1/2$  “head” atom is coherently transported between lattice sites via the lattice polarization. This polarization-dependent “Archimedes’ screw” transport at magic wavelength takes advantage of the vanishing vector polarizability of the scalar,  $J = 0$ , clock states of bosonic isotopes of divalent atoms. The on-site interactions between the clock atoms and the head atom are used to engineer entanglement.

A schematic of the entanglement process is presented in the Fig. The transport lattice is created by a superposition of two displaced circularly polarized standing wave lattices:  $\sigma_+$  and  $\sigma_-$  lattices. (a) A single head atom (orange circle) and several clock atoms (blue circles) are trapped in the minima of a 1-D optical lattice, with one or fewer atoms per site. Due to an intensity differential of the underlying lattices, the clock atoms couple strongly to the  $\sigma_+$  lattice (solid blue line). The head atom is placed in a superposition of atomic states: one which couples strongly to the  $\sigma_+$  lattice and one which couples strongly to the  $\sigma_-$  lattice (dashed orange line). (b) As  $\phi$  is increased, the latter state spatially separates and is transported along the lattice. (c) This portion of the head atom is then brought into contact with a clock atom to entangle the two atoms. (d) The head atom is transported further to obtain entanglement with the remaining clock atoms in a similar manner.



Many of the usual requirements for producing highly-entangled states between atoms – such as single-site addressability, single-site readout, and unity site occupation – are absent in this scheme. For a conservative choice of parameters, one would be able to put  $\sim 10^3$  clock atoms (Sr) into the maximally entangled GHZ state with high probability. This would enable a reduction in the projection noise of lattice clocks.

Details may be found in the paper: Jonathan D. Weinstein, Kyle Beloy, and Andrei Derevianko, *Phys. Rev. A* **81**, 030302(R) (2010).

## Giant coherence times in a trapped atomic gas

C. Deutsch<sup>1</sup>, F. Ramirez-Martinez<sup>2</sup>, C. Lacroûte<sup>2,4</sup>, W. Mainault<sup>2</sup>, F. Reinhard<sup>1,5</sup>,  
J.N. Fuchs<sup>3</sup>, F. Piéchon<sup>3</sup>, F. Laloë<sup>1</sup>, J. Reichel<sup>1</sup>, P. Rosenbusch<sup>2</sup>,

<sup>1</sup>*LKB - Ecole Normale Supérieure - UPMC - CNRS - Paris, France*

<sup>2</sup>*SYRTE - Observatoire de Paris - UPMC - CNRS - Paris, France*

<sup>3</sup>*Laboratoire de Physique des Solides- Université Paris-Sud - CNRS - Orsay, France*

<sup>4</sup>*present adress: California Institute of Technology, Pasadena, CA*

<sup>5</sup>*present adress: Physikal. Institut, Universität Stuttgart, Germany*

We report on the observation of very long coherence times on ultracold trapped <sup>87</sup>Rb atoms. The experiment<sup>1</sup> is designed to operate a microwave atomic clock in the  $10^{-13}$  s<sup>-1/2</sup> stability regime in a compact setup. We apply a two photon transition to the magnetically trappable states  $|F, m_F\rangle = |1, -1\rangle$  and  $|2, 1\rangle$ . The collisional shift is compensated by tuning the second order Zeeman shift below the magic field of 3.23G. Remaining field inhomogeneities limit the frequency spread to  $< 80$ MHz giving rise to dephasing of the individual atoms on a timescale of 2 to 3 s.<sup>2</sup>

Surprisingly the coherence time, measured by varying the Ramsey free evolution time, is  $58\text{s} \pm 12\text{s}$  and thus at least an order of magnitude larger than expected.

We explain this by a constant rephasing of the atomic spins driven by the Identical Spin Rotation Effect<sup>3</sup> that acts analogous to a continous spin echo. We demonstrate this effect by tuning the atom density and thereby the ISRE rate<sup>4</sup>. With increasing atom densities revivals of the fringe contrast are demonstrated.

The effect is very general in nature and should be observable in a multitude of systems.

<sup>1</sup>C. Lacroûte, F. Reinhard, F. Ramirez-Martinez, C. Deutsch, T. Schneider, J. Reichel, P. Rosenbusch IEEE Transaction on Frequency Control 2010 **56**, 106

<sup>2</sup>P. Rosenbusch, Phys. Rev. A **95**, 227 (2009)

<sup>3</sup>F. Piéchon, J. N. Fuchs, F. Laloë Phys. Rev. Lett. **102**, 215301 (2009)

<sup>4</sup>C. Deutsch, F. Ramirez-Martinez, C. Lacroûte, F. Reinhard, T. Schneider, J. N. Fuchs, F. Piéchon, F. Laloë, J. Reichel, P. Rosenbusch arXiv:1003.5925v1

# Towards a lattice based neutral magnesium optical frequency standard

W. Ertmer<sup>1</sup>, J. Friebe<sup>1</sup>, M. Riedmann<sup>1</sup>, A. Pape<sup>1</sup>, T. Wübbena<sup>1</sup>, A. Kulosa<sup>1</sup>,  
H. Kelkar<sup>1</sup>, E. Rasel<sup>1</sup>, O Terra<sup>2</sup>, K Predehl<sup>2</sup>, T Feldmann<sup>2</sup>, T Legero<sup>2</sup>, B Lipphardt<sup>2</sup>,  
G Grosche<sup>2</sup>, H Schnatz<sup>2</sup>,

<sup>1</sup>*Institute of Quantum Optics, Leibniz University Hannover, Hannover, Germany*

<sup>2</sup>*Physikalisch-Technische Bundesanstalt, Braunschweig, Germany*

Magnesium is an interesting candidate for a future high performance neutral atom optical frequency standard. It offers low sensitivity to frequency shifts of the  $^1S_0$  to  $^3P_0$  clock transition by room temperature blackbody radiation and several isotopes of suitable abundance (two bosonic, one fermionic) to realize an optical clock. In order to reach long spectroscopic times and therefore high resolution, it is necessary to perform spectroscopy on optically trapped atoms. For neutral atom optical clocks, it is possible to trap atoms in an optical lattice at the magic wavelength, where both states of the clock transition experience the same light shift due to the trapping field and can also be confined to the Lamb-Dicke regime. In this contribution, we report on the recent progress on the neutral atom magnesium frequency standard. We established a 73 km fiber link, which connects the Mg experiment (IQ, Hannover) to the Physikalisch-Technische Bundesanstalt (PTB, Braunschweig) to enable the comparison of the Mg frequency standard to PTBs high performance optical frequency standards. With this fiber link, we compared two ultrastable lasers at IQ and PTB on the  $10^{-15}$  level in fractions of a second. This fiber link was also used to determine the stability and absolute frequency of the current setup of the Mg frequency standard, which probes cold free falling atoms on the  $^1S_0$  to  $^3P_1$  transition. On the other hand, we are studying trapping of Mg in an optical dipole trap as a step towards a lattice-based frequency standard. Atoms are pre-cooled in a two-stage MOT. The second MOT has a decay channel to the dark  $^3P_0$  state. All cooling stages are running continuously and atoms are accumulated in a 1064 nm optical trap. Routinely, we trap up to  $10^5$  atoms at a temperature below 100 K with this technique. In the next step, we plan to implement an optical lattice and measure the value of the magic wavelength, which is theoretically predicted at 470 nm.

# Frequency measurement of the $4s^2S_{1/2} - 3d^2D_{5/2}$ transition of a single laser-cooled $^{40}\text{Ca}^+$ ion

Qu Liu, Yao Huang, Bin Guo, Jian Cao, Baoquan Ou, Wancheng Qu, Hua Guan, Xue-ren Hang and Ke-lin Gao<sup>†</sup>

*State Key Laboratory of Magnetic Resonance and Atomic and Molecular Physics, Wuhan Institute of Physics and Mathematics, Chinese Academy of Sciences, Wuhan 430071*

The optical clock based on a single  $^{40}\text{Ca}^+$  ion is one of the candidates for the next generation frequency standard<sup>1,2</sup>. The trapping and laser cooling  $^{40}\text{Ca}^+$  ion on the way towards optical frequency standards has been developed in our group<sup>3</sup>.

A single  $^{40}\text{Ca}^+$  ion was trapped in a miniature Paul trap. An RF drive voltage of 400 V<sub>p-p</sub> at frequency 10 MHz is applied to the ring as the electric trapping field. The cooling and repumping lasers (397 nm and 866 nm) locked to the commercial F-P cavity were referenced to the ultra stable clock laser by the home-made transfer cavity. A commercial Ti: Sapphire laser and one home-build diode laser at 729 nm are locked to two high-finesse ULE cavities separately by the PDH method. The beat frequency measurement result shows that the linewidth of the two lasers is around 50Hz<sup>4</sup>. In addition, an 854nm laser is used for returning the ion from the meta-stable  $^2D_{5/2}$  level.

The single ion fluorescence line shape signal is optimized by minimizing the excess micromotion<sup>5</sup>. A typical fluorescence signal counting rate of 12000 s<sup>-1</sup> was obtained for the single cold  $^{40}\text{Ca}^+$  ion which can survive overnight without cooling lasers now. The line width of single ion fluorescence signal is about 30 MHz.

The three magnet coil pairs aligned along three perpendicular directions (PMT, laser beam and vertical) are set to generate an arbitrary strength of the magnetic field. The full Zeeman profile components of the clock transition are achieved by counting the number of the quantum jumps observed in a fixed time period at different frequency. The measured linewidth of  $\Delta m_J = 0$  components is 200Hz. The center frequency of  $^{40}\text{Ca}^+$   $4s^2S_{1/2} - 3d^2D_{5/2}$  optical clock transition were measured by a fs comb system referenced to a standard hydrogen maser. And we lock the 729 nm laser system to atomic transition with four points locking method.

This work is supported by the National Basic Research Program of China (No. 2005CB724502), the National Natural Science Foundation of China (No. 10874205 and 10774161) and Chinese Academy of Sciences.

<sup>†</sup>email: klgao@wipm.ac.cn.

<sup>1</sup>M. Chwalla et al., *Phy. Rev. Lett.* 102, 023002 (2009)

<sup>2</sup>K. Matsubara et al., *Appl. Phys. Express* 1,067011 (2008)

<sup>3</sup>Shu Hua-Lin, et al., *Chin. Phys. Lett.*22, 1217 (2005), Guo Bin et al., *Front. Phys. China* 4, 144 (2009)

<sup>4</sup>Hua Guan, et al., A 729 nm laser with ultra-narrow linewidth for probing  $4s^2S_{1/2} - 3d^2D_{5/2}$  clock transition of  $^{40}\text{Ca}^+$  (submit to *Opt. Commun.*)

<sup>5</sup>Bin Guo et al., Minimization of excess micromotion to observe the ten Zeeman components of the quadrupole transition (submit to *J. Phys. B*)

# Decoherence and Collisional Frequency Shifts

Kurt Gibble<sup>1,2</sup>

<sup>1</sup>*The Pennsylvania State University, University Park, PA, USA*

<sup>2</sup>*SYRTE, Observatoire de Paris, Paris, France*

Decoherence of trapped gases makes the otherwise identical particles distinguishable. The distinguishability of particles has been controversial because several experiments have observed that particles appear spectroscopically identical in the presence of decoherence<sup>1,2</sup>. This has led to an argument that even distinguishable fermions could not produce a collision shift, but recently a shift was observed in a fermion lattice clock<sup>3</sup>. We offer an explanation of these experiments based on singlet and triplet states of colliding particles<sup>4</sup>. We will discuss the shifts for clocks, the relevance of mean field energies, and the relation to other recent treatments<sup>5,6</sup>.

---

<sup>1</sup>D. M. Harber *et al.*, Phys. Rev. A **66**, 053616 (2002).

<sup>2</sup>M. W. Zwierlein *et al.*, Phys. Rev. Lett. **91**, 250404 (2003).

<sup>3</sup>G. K. Campbell *et al.*, Science **324**, 360-363 (2009).

<sup>4</sup>K. Gibble, Phys. Rev. Lett. **103**, 113202 (2009).

<sup>5</sup>A. M. Rey, A.V. Gorshkov, and C. Rubbo, Phys. Rev. Lett. **103**, 260402 (2009).

<sup>6</sup>Z. Yu and C. J. Pethick, Phys. Rev. Lett. **104**, 010801 (2010).

# Reducing the Uncertainty due to Doppler Shifts to Improve the Accuracy of Cesium Clocks

J. Guna<sup>1</sup>, R. Li<sup>2</sup>, K. Gibble<sup>2</sup>, S. Bize<sup>1</sup>, A. Clairon<sup>1</sup>

<sup>1</sup>*SYRTE, Observatoire de Paris, Paris, France*

<sup>2</sup>*The Pennsylvania State University, University Park, PA, USA*

Doppler shifts are the largest source of uncertainty for some of the worlds most accurate cesium clocks<sup>1</sup>. The Doppler shifts arise due to phase variations in the microwave cavities, coupled with some motion of the atoms. There are phase variations in the cavities because the cavity has a finite Q the power fed into the cavity is absorbed by the walls. Therefore, there are small travelling waves in addition to the large standing wave, which results in phase variations throughout the cavity. To date, the uncertainties of clocks have been estimated using approximate or phenomenological expressions of the phase variations in the microwave cavity<sup>2</sup>.

Here we combine many measurements of the clock errors<sup>3</sup> with extensive finite element calculations of the phase variations<sup>4</sup> and their effects on the atoms<sup>5</sup>. The calculation relies on a Fourier expansion of axisymmetric finite element models which enables a full 3D solution from a short azimuthal Fourier series of 2D solutions. The Fourier field components,  $\cos(m\phi)$ , that contribute to the clock error,  $m = 0, 1$ , and 2, each have unique characteristics. We measure these characteristics for  $m = 0$  and 1, and find agreement with the calculations. This opens the path to dramatically reducing this source of error and improving the accuracy of the clocks. In addition, we have used the models to design improved cavities that produce negligible Doppler shifts for future clocks.

---

<sup>1</sup>See for example J. Guna *et al.*, IEEE Trans. on UFFC, **57**, 647-653, 2010; V Gerginov *et al.*, Metrologia **47**, 65-79 (2010).

<sup>2</sup>A. Khursheed *et al.*, IEEE Trans. UFFC **43**, 201-210 (1996); R. Schrder *et al.*, IEEE Trans. UFFC **49**, 383-392 (2002); S. Jefferts *et al.*, IEEE Trans. UFFC **52**, 2314-2321 (2005).

<sup>3</sup>F. Chapelet *et al.*, Proceedings of the 2006 EFTF, (2006).

<sup>4</sup>R. Li and K. Gibble, Metrologia **41**, 376-386 (2004).

<sup>5</sup>R. Li and K. Gibble, Proc. 2005 Freq. Control Symp., 99-104 (2005).

## Development of a strontium optical lattice clock at NPL

I.R. Hill<sup>1,2</sup>, E.M. Bridge<sup>1,3</sup>, Y.B. Ovchinnikov<sup>1</sup> G.P. Barwood<sup>1</sup> E.A. Curtis<sup>1,2</sup>  
P. Gill<sup>1,2,3</sup>

<sup>1</sup>*National Physical Laboratory, Hampton Road, Teddington, Middlesex, UK*

<sup>2</sup>*Blackett Laboratory, Imperial College, Prince Consort Road, London, UK*

<sup>3</sup>*Clarendon Laboratory, University of Oxford, Parks Road, Oxford, UK*

Frequency standards based on optical transitions show great potential as next generation clocks and have already demonstrated fractional frequency instabilities and uncertainties below the current caesium fountain microwave primary frequency standard<sup>1,2,3</sup>. One such candidate for a future redefinition of the second is the  $^1S_0 - ^3P_0$  clock transition in neutral strontium at 698 nm. Recent measurements of this transition at three national laboratories around the world have fractional frequency uncertainties in the  $10^{-15}$  range and agree to within a hertz<sup>4,5,6</sup>.

At the National Physical Laboratory we are developing a lattice clock arrangement to study and address systematic frequency shifts of the  $^1S_0 - ^3P_0$  clock transition of neutral strontium confined in a 1D optical lattice trap tuned to the ‘magic’ wavelength<sup>7</sup>. Our compact experimental system includes a novel Zeeman slower based on an array of discrete neodymium permanent magnets<sup>8</sup>. It requires no additional power supply or water-cooling and the spatial distribution of its magnetic field can be adjusted in-situ. The slower is characterised by measurement of the velocity distribution of atoms at the exit of the slower.

In order to probe the narrow linewidth clock transition optimally, a laser with sub-hertz linewidth is desirable. We have two identical, independent probe laser systems, which enable us to determine the linewidth via beat note detection. Each laser system consists of an extended cavity diode laser at 698 nm stabilised to a high finesse, vibrationally insensitive, vertically oriented, ULE Fabry-Perot cavity via Pound-Drever-Hall locking. The laser, optics and cavity are mounted on an active vibration isolation platform on the floor of an acoustically isolated, temperature stabilised room.

We present recent progress towards the NPL lattice clock with emphasis on narrow linewidth cavity stabilised lasers and cold atom source.

---

<sup>1</sup>T. Rosenband *et al.*, “Frequency Ratio of  $Al^+$  and  $Hg^+$  Single-Ion Optical Clocks; Metrology at the 17th Decimal Place”, *Science* **319**, 1808 (2008)

<sup>2</sup>A.D. Ludlow *et al.*, “Sr Lattice Clock at  $1 \times 10^{-16}$  Fractional Uncertainty by Remote Optical Evaluation with a Ca Clock”, *Science* **319**, 1805 (2008)

<sup>3</sup>C.W. Chou *et al.*, “Frequency Comparison of Two High-Accuracy  $Al^+$  Optical Clocks”, *Phys. Rev. Lett.* **104**, 070802 (2010)

<sup>4</sup>G.K. Campbell *et al.*, “The absolute frequency of the  $^{87}Sr$  optical clock transition”, *Metrologia* **45**, 539-548 (2008)

<sup>5</sup>X. Baillard *et al.*, “An optical lattice clock with spin-polarized  $^{87}Sr$  atoms”, *Eur. Phys. J. D*, **48**, 11-17 (2007)

<sup>6</sup>F.L. Hong *et al.*, “Measuring the frequency of a Sr optical lattice clock using a 120 km coherent optical transfer”, *Opt. Lett.*, **34**, 692-694 (2009)

<sup>7</sup>H. Katori *et al.*, “Ultrastable Optical Clock with Neutral Atoms in an Engineered Light Shift Trap”, *Phys. Rev. Lett.* **91**, 173005 (2003)

<sup>8</sup>Y.B. Ovchinnikov, “A Zeeman slower based on magnetic dipoles”, *Opt. Commun.* **276**, 261-267 (2007)

## Electron Impact Excitation of Si Ions (XII–XIV)

K.M. Aggarwal, F.P. Keenan

*Astrophysics Research Centre, School of Mathematics and Physics,  
Queen's University, Belfast BT7 1NN, Northern Ireland, UK*

Emission lines of Si ions, including those from Si XII–XIV, have been observed in a variety of astrophysical plasmas and are useful for temperature and density diagnostics. Additionally, observations from the x-ray satellite *Chandra* have also revealed many emission lines from Si ions, and have been helpful in studies of accretion powered sources, such as active galaxies. However, to analyse observations and to understand the physical mechanisms in astronomical sources, atomic data are required for a variety of parameters, such as energy levels, radiative rates (A-values), and excitation rates or equivalently the effective collision strengths ( $\Upsilon$ ), which are obtained from the electron impact collision strengths ( $\Omega$ ). Such data are also useful for the modelling of fusion plasmas. Therefore, in this paper we report our calculations for Si XII, Si XIII and Si XIV.

Experimentally, energy levels have been compiled by NIST and are available at their website <http://physics.nist.gov/PhysRefData>. Theoretically, energy levels and A-values are available<sup>1</sup> for transitions for 15 Li-like ions in the  $6 \leq Z \leq 28$  range. Similar data for He-like Si XIII are also available<sup>2,3</sup> for transitions among the lowest 14 levels of the  $n \leq 4$  configurations. For H-like Si XIV, energy levels and A-values have been calculated by Pal'chikov<sup>4</sup> and Jitrik and Bunge<sup>5</sup>. However, collisional atomic data for these ions<sup>6–8</sup> are very limited. Therefore, in this paper we report a complete set of results (namely energy levels, radiative rates and effective collision strengths) for all transitions among the lowest 24, 49 and 25 levels of Si XII, Si XIII and Si XIV, respectively. These levels belong to the  $n \leq 5$  configurations. Additionally, we also provide the A-values for four types of transitions, namely electric dipole (E1), electric quadrupole (E2), magnetic dipole (M1), and magnetic quadrupole (M2), because these are also required for plasma modelling. For our calculations we employ the fully relativistic GRASP code for the determination of wavefunctions, and the DARC code for the calculations of collision strengths ( $\Omega$ ) over a wide energy range. Resonances in the thresholds region have been resolved in a fine energy mesh to obtain the effective collision strengths ( $\Upsilon$ ) over a wide temperature range below  $10^7$  K, suitable for applications in a variety of plasmas. Detailed data along with comparisons will be presented during the conference.

*This work has been financed by the EPSRC and STFC of the United Kingdom.*

---

<sup>1</sup>Nahar S N 2002 *Astron. Astrophys.* **389** 716, <sup>2</sup>Porquet D and Dubau J 2000 *Astron. Astrophys. Suppl.* **143**, 495, <sup>3</sup>Delahaye F, Pradhan A K and Zeippen C J 2006 *J. Phys.* **B39** 3465, <sup>4</sup>Pal'chikov V G 1998 *Phys. Scr.* **57** 581, <sup>5</sup>Jitrik O and Bunge C F 2004 *J. Phys. Chem. Ref. Data* **33** 1059, <sup>6</sup>Zhang H L, Sampson D H and Fontes C J 1990 *At. Data Nucl. Data Tables* **44** 31, <sup>7</sup>Zhang H and Sampson D H 1987 *Astrophys. J. Suppl.* **63**, 487, <sup>8</sup>Aggarwal K M and Kingston A E 1992 *Phys. Scr.* **46** 193

## Electron Impact Excitation of C V

K.M. Aggarwal<sup>1</sup>, T. Kato<sup>2</sup>, F.P. Keenan<sup>1</sup>, I. Murakami<sup>2</sup>

<sup>1</sup>*Astrophysics Research Centre, School of Mathematics and Physics,  
Queen's University, Belfast BT7 1NN, Northern Ireland, UK*

<sup>2</sup>*National Institute for Fusion Science, Oroshi-cho, Toki, Gifu, 509-5292 Japan*

Emission lines from several ionisation stages of carbon, including He-like C V, have been observed in solar plasmas<sup>1</sup>. The  $n = 2$  lines in the x-ray region (namely, the resonance  $1s^2\ ^1S_0 - 1s2p\ ^1P_1^o$ , intercombination  $1s^2\ ^1S_0 - 1s2p\ ^3P_1^o$ , and forbidden  $1s^2\ ^1S_0 - 1s2p\ ^3S_1$ ) have particularly been observed in the Sun from rockets and satellites, and are useful for the determination of electron densities and temperatures in the solar corona and transition region<sup>2</sup>. Similarly, lines of C V in the EUV range have recently been measured by Kato et al.<sup>3</sup> in fusion plasmas from Large Helical Device (LHD) as carbon is one of the main impurities in fusion reactors. However, to analyse observations, atomic data are required for a variety of parameters, such as energy levels, radiative rates (A-values), and excitation rates or equivalently the effective collision strengths ( $\Upsilon$ ), which are obtained from the electron impact collision strengths ( $\Omega$ ). Experimentally, only energy levels are available for C V (<http://physics.nist.gov/PhysRefData>). Similarly, A-values are also available for many (electric dipole) transitions on the NIST and CHIANTI websites, but collisional atomic data for C V are restricted to transitions only from the lowest three levels to higher excited levels<sup>4</sup>. These calculations of Sampson et al.<sup>4</sup> are based on the hydrogenic approximation and do not include the contribution of resonances, which can be very important for an ion such as C V. Therefore, in this paper we report a complete set of results (namely energy levels, radiative rates, lifetimes, and effective collision strengths) for all transitions among the lowest 49 levels of C V. These levels belong to the  $1s^2$ ,  $1s2\ell$ ,  $1s3\ell$ ,  $1s4\ell$ , and  $1s5\ell$  configurations. Finally, we also report the A-values for four types of transitions, namely electric dipole (E1), electric quadrupole (E2), magnetic dipole (M1), and magnetic quadrupole (M2), because these are also required for plasma modelling.

For the determination of wavefunctions we employ the fully relativistic GRASP code, and for the calculations of  $\Omega$ , the *Dirac atomic R-matrix code* (DARC) of P.H. Norrington and I.P. Grant. Collision strengths and effective collision strengths are calculated for all 1176 transitions among the 49 levels of the  $n \leq 5$  configurations over a wide energy (temperature) range up to 42 Ryd ( $7 \times 10^5$  K), suitable for applications in a variety of plasmas. Additionally, parallel calculations have also been performed with the *Flexible Atomic Code* (FAC) of Gu<sup>5</sup>, so that all atomic parameters can be rigorously assessed for accuracy. Detailed data along with comparisons will be presented during the conference.

*This work has been financed by the EPSRC and STFC of the UK and NIFS, Japan.*

<sup>1</sup>Dere K P, Landi E, Young P R and Del Zanna G. 2001, ApJS, 134, 331, <sup>2</sup>Doyle J G 1980, A&A, 87, 183,

<sup>3</sup>Kato T et al. 2009, J. Phys. Conf. Series, 163, 012101, <sup>4</sup>Sampson D H, Goett S J and Clark R E H 1983, ADNDT, 29, 467, <sup>5</sup>Gu M F 2003, ApJ, 582, 1241.

## ***s*-wave scattering by an absorbing nanowire**

Martin Fink<sup>a</sup>, Andrés Naranjo<sup>b</sup>, Florian Arnecke<sup>a</sup>, Johannes Eiglsperger<sup>a</sup>,  
Harald Friedrich<sup>a</sup>, Javier Madroñero<sup>a</sup>, Patrick Raab<sup>a</sup>, Andreas Wirzba<sup>c</sup>

<sup>a</sup>*Physik Department, Technische Universität München, 85747 Garching, Germany*

<sup>b</sup>*Facultad de Ciencias, Universidad Nacional, Medellín, Colombia*

<sup>c</sup>*Institute for Advanced Simulation and Institut für Kernphysik, Forschungszentrum Jülich, 52425 Jülich, Germany*

The scattering of a cold atom (or molecule) by an infinite cylindrical conducting wire is a highly nontrivial problem, because it is effectively two-dimensional and:

(i) in contrast to effectively 1D systems and to 3D systems with radial symmetry, the interaction potential does not have a simple structure; (ii) scattering theory in 2D differs significantly from 3D scattering, in particular near threshold.<sup>1</sup>

For a spherical atom of mass  $M$  at distance  $r$  from the axis of a cylindrical wire of radius  $R$ , the nonretarded atom-wire potential is <sup>2</sup>

$$V(r) = -\frac{\hbar^2}{2M} \frac{\beta}{r^3} X\left(\frac{r}{R}\right), \quad \beta = \frac{2M}{\hbar^2} \langle \hat{d}_i^2 \rangle, \quad (1)$$

where  $\langle \hat{d}_i^2 \rangle$  is the expectation value of one component of the dipole operator squared, and  $X$  is a universal function of  $r/R$ . Values of  $\beta$  range from a few thousand atomic units for the ground-state hydrogen atom to several million a.u. for the heavier alkalis. The 2D radial Schrödinger equation is solved with the potential (1) and incoming boundary conditions near  $r = R$ , corresponding to total absorption near the surface of the wire. The complex  $s$ -wave scattering length  $\mathbf{a}$  strictly obeys a scaling rule:  $\mathbf{a} = R \tilde{\mathbf{a}}(R/\beta)$ , and its real and imaginary parts are shown as functions of  $R/\beta$  in Fig. 1.  $\mathbf{a}$  determines the near-threshold behaviour of the scattering and absorption cross sections which diverge as  $k^{-1} \left( [\ln(k|\mathbf{a}|/2) + \gamma_E]^2 + [\arg(\mathbf{a}) - \frac{\pi}{2}]^2 \right)^{-1}$  for  $E = \hbar^2 k^2 / (2M) \rightarrow 0$ .

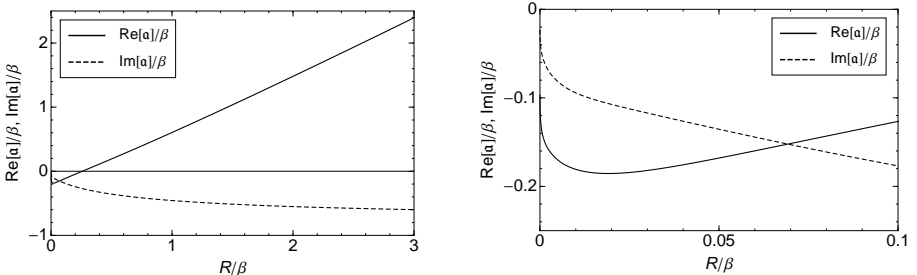


Figure 1: Real and imaginary parts of the complex  $s$ -wave scattering length  $\mathbf{a}$ .

This is the first calculation of the scattering of a polarizable atom by a conducting wire, which is based on a theoretically founded atom-wire potential and the 2D nature of the problem. A more detailed account is to be published shortly.<sup>3</sup>

<sup>1</sup>F. Arnecke, H. Friedrich, P. Raab, Phys. Rev. A **78** (2008) 052711.

<sup>2</sup>C. Eberlein, R. Zietal, Phys. Rev. A **75** (2007) 032516.

<sup>3</sup>M. Fink *et al.*, Phys. Rev. A, accepted for publication.

## Series of doubly-excited states $^1S^e$ and $^3S^e$ of $Be^{2+}$ below the $N=2$ threshold of $Be^{3+}$ \*

T. T. Gien<sup>+</sup>

<sup>+</sup>*Department of Physics and Physical Oceanography, Memorial University of Newfoundland, St. Johns, NL, A1B 3X7 Canada*

We report the results of our determination of the series of S wave singlet doubly-excited states  $^1S^e$  as well as those of S wave triplet doubly excited states  $^3S^e$  of  $Be^{2+}$  below the  $N=2$  excitation threshold of  $Be^{3+}$ , employing a numerical procedure prescribed by us<sup>1</sup>. This procedure was based on an accurate calculation of phase shifts for electron- $Be^{3+}$  elastic scattering using the Harris-Nesbet variational method<sup>2</sup>. Accurate results of position and width of these doubly excited state resonances were determined, including those lying very close to the  $N=2$  threshold of  $Be^{3+}$  which usually stay very close to each other and have very small widths and are, thereby, very difficult to be determined.

For the S-wave singlet doubly excited states  $^1S^e$ , we succeeded in determining altogether 21 of these doubly excited states, 11 belonging to the a-series denoted by  $^1S^e(2,2a)$  -  $^1S^e(2,12a)$  and 10 belonging to the b-series denoted by  $^1S^e(2,2b)$  -  $^1S^e(2,11b)$ . For the S-wave triplet doubly excited states  $^3S^e$ , we also found altogether 20 of these doubly excited state resonances, 10 belonging to the a-series denoted by  $^3S^e(2,3a)$  -  $^3S^e(2,12a)$  and 10 belonging to the b-series denoted by  $^3S^e(2,3b)$  -  $^3S^e(2,12b)$ . We succeeded as well in presenting explicitly in graphical forms all the 41 doubly excited states determined by us. These graphical presentations help in confirming the definite existence of these doubly excited state resonances in the energy distributions of phase shifts and cross sections of electron- $Be^{3+}$  scattering.

Detailed description of this work and its complete results including the positions and widths of all these 41 doubly excited states determined by us as well as their graphical presentations will be reported at the conference with discussion. Comparison of our results of position and width with those obtained by other research groups for a few lowest-lying of these doubly-excited-state resonances will be made.

\*This research work is supported by the NSERC of Canada

---

<sup>1</sup> See for example T T Gien, J Phys B **43**, 025202 (2010), and other references therein

<sup>2</sup>R.K. Nesbet, *Variational Method in Electron-Atom Scattering Theory* (New York: Plenum 1980)

# Strong-force effects in cold antiproton-atom collisions

G. F. Gribakin

*School of Mathematics and Physics, Queen's University, Belfast, UK*

Following the method used for cold atom-atom collisions<sup>1</sup>, the following expression can be obtained for antihydrogen-atom scattering length,<sup>2</sup>

$$a = \bar{a} \left[ 1 - \tan \left( \Phi - \frac{\pi}{2(n-2)} - \frac{\pi}{2} + \delta_{\text{sf}} \right) \tan \left( \frac{\pi}{n-2} \right) \right], \quad (2)$$

where  $\bar{a}$  is the *mean* scattering length<sup>1</sup>,  $\Phi = \int_0^\infty \sqrt{-2mU(R)}dR$  is the semiclassical phase at zero energy,  $m$  is the reduced mass,  $R$  is the antiproton-nuclear distance,  $U(R)$  is the antihydrogen-atom potential energy ( $\propto R^{-n}$  with  $n = 6$  at large  $R$ ),  $\delta_{\text{sf}}$  is the phaseshift due to the strong force between the antiproton and the nucleus:  $\tan \delta_{\text{sf}} = -2\pi a_{\text{sf}}/a_c \equiv -\tilde{a}_{\text{sf}}$ ,  $a_{\text{sf}}$  is the strong-force scattering length, and  $a_c = (mZ)^{-1}$  is the Coulomb length (we use atomic units). Due to antiproton annihilation  $a_{\text{sf}}$  is complex.

For antiproton ( $\bar{p}$ ) collisions with atoms,  $U(R) \simeq -\frac{1}{2}\alpha_d e^2 R^{-4}$  at large  $R$ , where  $\alpha_d$  is the atomic dipole polarisability. In this case  $n = 4$  and Eq. (1) takes the form

$$a = -\bar{a}_4 (\tan \Phi_4 - \tilde{a}_{\text{sf}}) (1 + \tilde{a}_{\text{sf}} \tan \Phi_4)^{-1}, \quad (3)$$

where  $\bar{a}_4 = \sqrt{\alpha_d m}$  and  $\Phi_4 = \Phi - \frac{3\pi}{4}$ . For  $\bar{p}$ -He,  $a_{\text{sf}} = 1.851 - 0.630i$  fm.<sup>3</sup> Figure 1 shows the reduced scattering length  $a/\bar{a}_4$  as a function of the phase  $\Phi_4$  (mod  $\pi$ ) calculated with and without the strong-force effect. Using two  $\bar{p}$ -He potentials,<sup>4</sup> one finds  $\Phi_4 = 161.467$  and  $162.870$ , yielding  $a = -33.5 - 10.8i$  and  $76.3 - 28.8i$ , respectively. Hence, one obtains quite different estimates of the antiproton annihilation cross section from  $\sigma_a = 4\pi |\text{Im } a|/k$ , where  $k$  is the collision wave number.

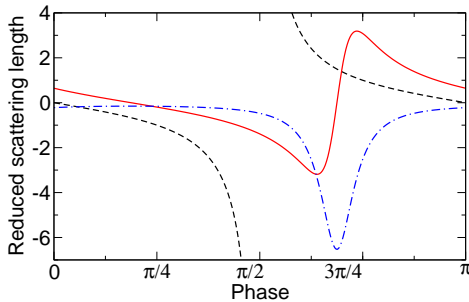


Figure 1: *Reduced scattering length as a function of the phase  $\Phi_4$ : dashed curve, for  $\tilde{a}_{\text{sf}} = 0$ ; solid and chain curves,  $\text{Re } a/\bar{a}_4$  and  $\text{Im } a/\bar{a}_4$ , respectively, for  $\bar{p}$ -He collisions.*

<sup>1</sup>G. F. Gribakin and V. V. Flambaum, Phys. Rev. A **48**, 546 (1993).

<sup>2</sup>A. Thompson, G. F. Gribakin and S. Jonsell, unpublished; A. Thompson, MPhil thesis, Queen's University Belfast (2009).

<sup>3</sup>S. Jonsell, Nucl. Instrum. Methods Phys. Res. B **247**, 138 (2006).

<sup>4</sup>W. R. Gibbs, Phys. Rev. A **56**, 3553 (1997); A. C. Todd and E. A. G. Armour, J. Phys. B **38**, 3367 (2005).

# Properties of decaying Feshbach resonances

Thomas M. Hanna, Eite Tiesinga, Paul S. Julienne

*Joint Quantum Institute, University of Maryland and NIST,  
100 Bureau Drive Stop 8423, Gaithersburg MD 20899-8423, USA.  
thomas.hanna@nist.gov*

Feshbach resonances, a vital control tool for ultracold atomic gases, usually have some inherent decay mechanisms. This is also expected to be the case for resonances in scattering of ultracold ground state molecules. We study the properties of decaying Feshbach resonances tuned by magnetic fields and/or RF radiation. We discuss different mechanisms of decay, and situations in which these resonances can be useful. One focus is resonances in  ${}^6\text{Li}$ - ${}^{40}\text{K}$ , in which decay via coupling to higher partial waves is suppressed by a centrifugal barrier. RF used to couple a colliding pair to a bound state typically also couples a large number of exit channels<sup>1</sup>. The resulting loss feature may be easily tuned in location and width, allowing its use as an RF knife for evaporative cooling<sup>2</sup> (see Fig. 1). Circular-polarised RF has the potential to create resonances without decay (dashed line in Fig. 1).

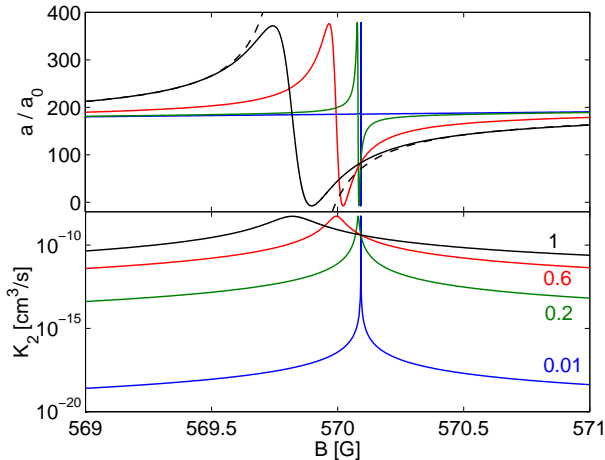


Figure 1: *Creation of a decaying resonance in  ${}^6\text{Li}$  using RF radiation. Scattering length  $a$  and two-body loss rate coefficient  $K_2$  are shown as a function of magnetic field  $B$ . The Rabi frequency of the RF, given in MHz, can be used to tune the resonance width.*

<sup>1</sup>T. M. Hanna *et al.*, *arXiv:1004.0636* (2010).

<sup>2</sup>L. Mathew *et al.*, *Phys. Rev. A* 80, 030702(R) (2009).

# High probability single atom occupancy in a microscopic dipole trap

A. Hilliard, T. Grünzweig, M. McGovern, M. F. Andersen,

*Jack Dodd Centre for Quantum Technology, Department of Physics, University of Otago, New Zealand*

Neutral atoms stored in optical traps are a strong candidate in the development of physical realizations of a quantum logic device. Far off-resonance optical traps provide conservative potentials and excellent isolation from the environment, and may be arranged to produce arrays of atoms in which the atoms' internal and external degrees of freedom may be tuned by applied electromagnetic fields<sup>1</sup>. Two-particle operations may then be realized through, for example, exciting the atoms in adjacent traps to Rydberg states and making use of the dipole interaction<sup>2</sup>.

One of the challenges associated with this approach is the reliable generation of single atom occupancy at each site in the array of dipole traps. A promising approach to solve this challenge is the use of light-assisted collisions. It has been observed that light-assisted collisions between atoms in a microscopic dipole trap can produce a mean occupancy of 0.5 - that is, either zero or one atom remaining in the trap<sup>3</sup>. However, the 50% success rate of the method in producing a single atom in the dipole trap limits its usefulness for arrays with more than a few sites.

Here we demonstrate that by using light-assisted collisions on a dipole trapped sample of atoms, we obtain 82.7% efficiency in the production of single atoms in the trap<sup>4</sup>. We form an optical dipole trap by passing 828 nm light through a high numerical aperture aspheric lens located inside a vacuum chamber<sup>3</sup>. We then induce light-assisted collisions using quasi-resonant light on the D1 and D2 lines of <sup>85</sup>Rb. The two-body light-assisted collision decay rate is isolated experimentally by beginning each run with only two atoms, whereupon we observe the decay into the one and zero atom states. The mechanism responsible for the efficient production of one atom states is a two body collision that leads to the expulsion of only one of the participants in the collision. In the absence of other loss mechanisms, this process leads to the deterministic preparation of single atoms in the dipole trap. We explore the process through a systematic study of the experimental parameters, and find that by appropriate tuning we can obtain a range of single atom loading efficiencies from the previously measured 50% to the improved value of 82.7%. To quantify the improvement, this method would enable us to probabilistically load 15 sites with single atoms in a time of seven seconds, whereas at 50% efficiency it would take approximately three and a half hours.

This work is supported by NZ-FRST Contract No. NERF-UOOX0703, and UORG.

<sup>1</sup>R. Dumke, M. Volk, T. Mütter, F. B. J. Buchkremer, G. Birkl, and W. Ertmer, *Phys. Rev. Lett.*, **89**, 097903 (2002).

<sup>2</sup>A. Gaëtan, Y. Miroshnychenko, T. Wilk, A. Chotia, M. Viteau, D. Comparat, P. Pillet, A. Browaeys, and P. Grangier, *Nature Physics*, **5**, 115 (2009); E. Urban, T. A. Johnson, T. Henage, L. Isenhower, D. D. Yavuz, T. G. Walker and M. Saffman, *Nature Physics*, **5**, 110 (2009).

<sup>3</sup>N. Schlosser, G. Reymond, I. Protsenko and P. Grangier, *Nature*, **411**, 1024 (2001).

<sup>4</sup>T. Grünzweig, A. Hilliard, M. McGovern and M. F. Andersen, *Under review in Nature Physics*.

# Stabilization of Helium in Intense Laser Fields

S. Askeland<sup>1</sup>, S.A. Sørngård<sup>1</sup>, R. Nepstad<sup>1</sup>, T. Birkeland<sup>2</sup>, M. Førre<sup>1</sup>

<sup>1</sup>*Department of Physics and Technology, University of Bergen, Bergen, Norway*

<sup>2</sup>*Department of Mathematics, University of Bergen, Bergen, Norway*

We investigate the impact of electron-electron correlations on the ionization dynamics of helium in intense, high-frequency laser fields by solving the time-dependent Schrödinger equation from first principles. This six dimensional problem calls for sophisticated computational tools. For this purpose we use the PyProp framework for parallel computations<sup>1</sup>. The stabilization phenomenon is explored for a range of laser frequencies and pulse durations. Although we observe a decrease in the total ionization yield at high field strengths, the hallmark of atomic stabilization<sup>2</sup>, the repulsion between the electrons has a detrimental effect on the degree of stabilization, in particular for short pulses<sup>3</sup>. Investigation of the ion channel yields reveals that the double ionization process is less prone to two-electron effects, and consequently exhibits the most distinct signature of stabilization. We also find that commonly used one-dimensional models tend to overestimate the effect of correlation.

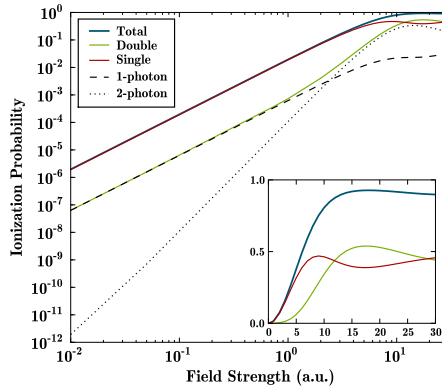


Figure 1: *Single, double and total ionization probability of helium in its ground state versus electric field strength  $E_0$  (in atomic units), for a 6-cycle laser pulse with  $\hbar\omega = 136$  eV ( $\omega = 5$  a.u.). Inset: same as above, but plotted on a linear scale. Dashed and dotted lines: corresponding one- and two-photon double ionization probabilities.*

<sup>1</sup>T. Birkeland and R. Nepstad, *Pyprop*, <http://pyprop.googlecode.com>

<sup>2</sup>J. H. Eberly and K. C. Kulander, *Science* **262**, 1229 (1993)

<sup>3</sup>T. Birkeland et al., *Phys. Rev. Lett.* **104**, 163002 (2010)

# Anharmonicity-driven dynamics of a cold atom cloud in a combined trap

A. Bertoldi<sup>1</sup>, L. Ricci<sup>2</sup>,

<sup>1</sup>*Institut d'Optique, Campus Polytechnique, F-91127 Palaiseau, France*

<sup>2</sup>*Dipartimento di Fisica, Università di Trento, I-38123 Trento-Povo, Italy*

We report on the behavior of cold Rb atoms trapped in an anharmonic gravito-magnetic potential. Remarkably, the position of the effective potential minimum is dependent on the initial temperature of the atomic ensemble. This effect is a consequence of the thermal nature of the sample and the anharmonicity of the combined potential. Besides a theoretical description, we carried out numerical simulations of the evolution of trapped clouds under different boundary conditions in terms of temperature and release position. Both theory and simulation are in good agreement with the experimental measurements obtained on cold atomic samples of  $^{87}\text{Rb}$  prepared at different temperatures. Possible applications of the observed behavior can be a novel technique to measure the temperature of a trapped atomic cloud, and a way to spatially separate thermal and condensed phases in BEC experiments.

# Composite pulses for three-state quantum systems

G.T. Genov, B.T. Torosov, N.V. Vitanov

*Department of Physics, Sofia University, James Bourchier 5 blvd, 1164 Sofia, Bulgaria*

Composite pulses are used in nuclear magnetic resonance<sup>1,2</sup>, and most recently, in trapped-ion quantum information processing<sup>3</sup>, for design of qubit rotations that are more robust against variations in the pulse area and/or the detuning than single resonant pulses of precise area. The composite pulse is a sequence of pulses with well defined relative phases between each other. The composite pulses can be considered as an alternative method to adiabatic pulses with similar robustness and higher fidelity.

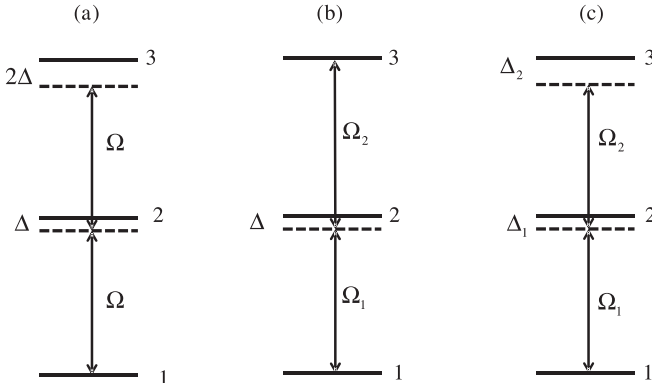


Figure 1: *Three-state chainwise connected quantum systems. (a) Same couplings, equidistant detunings. (b) Different couplings, zero two-photon detuning. (c) Different couplings and different detunings.*

In this work we describe the design of composite pulses for three-state chainwise connected quantum systems. These pulses can be used in three different situations depicted in Fig.1. For equal couplings and equidistant detunings, [Fig.1(a)], we use the Majorana decomposition<sup>4,5</sup> to reduce the dynamics to an effective two-state system, which allows us to find the three-state propagator analytically and use the pool of available composite pulses. For different couplings and two-photon resonance [Fig.1(b)], we use the Morris-Shore decomposition<sup>6</sup>, which again reduces the dynamics to an effective two-state problem and allows us to find the propagator analytically. Finally, in the general case of different couplings and different detunings [Fig.1(c)], we resort to numerical simulation<sup>7</sup>.

<sup>1</sup>M. H. Levitt, Prog. NMR Spectrosc. **18**, 61 (1986).

<sup>2</sup>S. Wimperis, J. Magn. Reson. **109**, 221 (1994).

<sup>3</sup>H. Häffner, C.F. Roos, and R. Blatt, Phys. Rep. **469**, 155 (2008).

<sup>4</sup>E. Majorana, Nuovo Cimento **9**, 43 (1932).

<sup>5</sup>F. Bloch and I. I. Rabi, Rev. Mod. Phys. **17**, 237 (1945).

<sup>6</sup>J. R. Morris and B. W. Shore, Phys. Rev. A **27**, 906 (1983).

<sup>7</sup>G.T. Genov, B.T. Torosov, and N.V. Vitanov, to be published

# Spin Nutation Induced by Atomic Motion in a Magnetic Lattice

A. Hatakeyama, Y. Kobayashi, Y. Shiraishi

*Tokyo University of Agriculture and Technology, Tokyo, Japan*

The coherent interactions of atoms or quantum systems with resonant electromagnetic radiation are of great importance in modern physics. They are widely used for preparing and detecting quantum states as required, providing indispensable techniques in many research fields, including rapidly progressing quantum information studies. The Rabi oscillation is a fundamental coherent phenomenon, where resonant monochromatic radiation exchanges the populations between atomic internal states periodically. The Rabi oscillation is observed when an ensemble of atoms is subjected to a sinusoidal oscillating perturbation from the radiation. This perturbation, however, can be realized without electromagnetic radiation. We here report coherent spin nutation by resonant excitation in an atomic beam not using electromagnetic radiation but using a periodic magnetostatic field (“magnetic lattice”) through which the atomic beam passes.

In the experiment an optically spin-polarized Rb atomic beam with a velocity of a few hundred m/s enters the magnetic lattice. The magnetic resonance occurs inside the lattice when the frequency of the periodic perturbation experienced by the atoms equals the transition frequency. The spatial period of the magnetic field is about 2 mm, and hence the frequency is on the order of hundred kHz, corresponding to the transitions between the ground state Zeeman sublevels that are split by an external dc field. The resultant population transfer is measured as a function of the strength of the periodic magnetic field after the atoms exit from the lattice.

The magnetic lattice is produced by some layers of the planar arrays of parallel current-carrying wires crossing the beam traveling region. This configuration, reminiscent of wire-chamber-type particle detectors, allows high beam transmission for a variety of incident angles, which was not attainable with our previous version of the magnetic lattice using a stack of printed circuit boards.<sup>1</sup> This degree of freedom of the incident angle is important to induce coherent excitation for an atomic ensemble; when the beam is incident parallel to the wire “planes” (the so-called channeling condition), the amplitude of the resonance frequency component of the oscillating field is larger for atoms traveling closer by the wire planes. In this case, the atoms in the beam experience different nutation frequencies depending on their incident positions and hence measured spin nutation signals quickly decay as an ensemble average. However, under the “oblique” incident conditions that the beam travels across the planes of the wires several times, the amplitude is independent of the incident position. This beam configuration thus enables coherent population transfer between the magnetic sublevels for the ensemble of atoms in the beam. Longer coherent oscillation in the spin nutation signals has actually been observed for the oblique incident beam than for the parallel incident one.

<sup>1</sup>Y. Kobayashi and A. Hatakeyama, “Magnetic resonance of atoms passing through a magnetic lattice”, J. Phys.: Conf. Ser. **185**, 012021 (2009).

# Non-dispersive matter wave packets in driven systems

K. A. Heenan<sup>1</sup>, M. Salerno<sup>2</sup>, T. J. Alexander<sup>1</sup>

<sup>1</sup>*ARC Centre of Excellence for Quantum-Atom Optics and Nonlinear Physics Centre, Research School of Physical Sciences and Engineering, The Australian National University, Canberra, ACT 0200, Australia*

<sup>2</sup>*Department of Physics, University of Salerno, Via S. Allende, I-84081 Baronissi (SA), Italy*

We study energy transfer to a Bose-Einstein condensate with an attractive interatomic interaction, in the presence of weak periodic driving. A ratchet effect has been found to occur in such systems<sup>1</sup>, however the underlying physical mechanisms of energy transfer are not well understood. We investigate, analytically and numerically, excitation of a bright soliton confined in a harmonic trap (see Figure 1a) and we identify the key physical mechanisms of energy transfer. Understanding the nature of energy transfer will have applications to controlling transport behaviour of matter wave solitons in more complex potentials.

We find that energy transfer occurs through two different physical mechanisms, in distinct regions of parameter space, as shown in Figure 1b. In the so-called ‘single particle’ regime, where the soliton behaves effectively as a classical particle, energy transfer occurs by parametric driving. In the presence of external trapping, coupling can occur between the mode of the trap and the width oscillations of the soliton, leading to a second mechanism for energy transfer (internal mode coupling).

We use this understanding of the fundamental mechanisms for energy transfer in a harmonic trap to describe the self-trapping and tunnelling behaviour of a soliton in a driven double-well or quasi-stable potential. Such analysis may predict the conditions under which controllable energy transfer can occur in experiments with ultracold atoms.

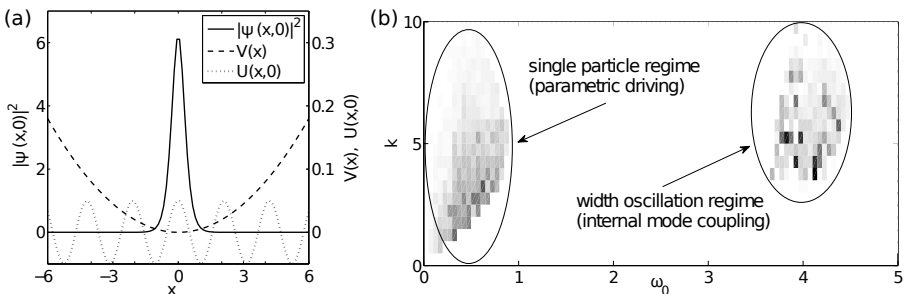


Figure 1: (a) Soliton subject to trapping  $V(x) = \frac{1}{2}\alpha^2 x^2$ , and driving  $U(x, t) = \eta \cos(kx) \cos(\omega_0 t)$ ,  $\alpha = 0.1$ ,  $\eta = 0.05$ ,  $k = 3$  (dimensionless variables). (b) Energy transfer to a driven soliton in a harmonic trap (white: no energy transfer; black: maximal energy transfer). Two regions corresponding to different energy transfer mechanisms are identified.

<sup>1</sup>Poletti, D. *et al.*, Phys. Rev. Lett. **101**, 150403 (2008).

# Localised matter wave excitations in an optical lattice

T.J. Alexander

*ARC Centre of Excellence for Quantum-Atom Optics and Nonlinear Physics Centre, Research School of Physical Sciences and Engineering, The Australian National University, Canberra, ACT 0200, Australia*

Optical lattices, periodic potentials formed from interfering laser beams, have proven to be powerful tools for the manipulation and control of Bose-Einstein condensates. A particularly dramatic effect is the possibility of self-localization of a condensate in a lattice linear band gap – even when the interparticle interactions are repulsive – due to the interplay between periodicity and condensate nonlinearity. This can even lead to the localization of the otherwise extended condensate nonlinear Bloch states <sup>1</sup>.

In this work I show theoretically, within the mean-field approximation, that nonlinear Bloch waves may be localized in almost arbitrary forms, even taking the form of “waveguides” through a two-dimensional lattice (see Fig. 1(a)). I reveal that these waveguides may support condensate flow in continuous wave form and suggest a scheme for the generation of these states using the single-site addressability techniques demonstrated in experiment <sup>2</sup>.

I show that the waveguides may support new types of localised nonlinear excitation such as the propagation of highly robust pulses or the appearance of density breathers. The pulses may interact with one another without change of shape or dependence on phase, and propagate around corners in a waveguide (see Fig. 1(a)). The breathers can appear following the breakdown of transverse oscillations of the waveguide (see Fig. 1(b)). These results suggest that in addition to providing a possible tool for manipulating and controlling the flow of a condensate precisely, these waveguide-like states provide an ideal environment for the investigation of nonlinear dynamical effects.

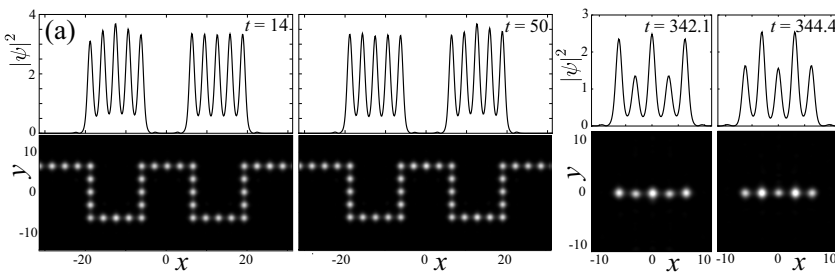


Figure 1: (a) A nonlinear Bloch wave truncated in the form of a waveguide, supporting the propagation of a self-localised pulse around the waveguide bends. (b) The emergence of a breather-like density excitation from transverse oscillations.

<sup>1</sup>T.J. Alexander, E.A. Ostrovskaya and Yu.S. Kivshar, Phys. Rev. Lett. **96**, 040401 (2006).

<sup>2</sup>P. Würtz, T. Langen, T. Gericke, A. Koglbauer, and H. Ott, Phys. Rev. Lett. **103**, 080404 (2009).

## <sup>85</sup>Rb Bose-Einstein condensates with tunable interactions

P.A. Altin, N.P. Robins, D. Döring, J.E. Debs, R. Poldy, C. Figl, J.D. Close,

*Australian Centre for Quantum Atom Optics, Australian National University, ACT  
0200, Australia*

The ability to tune the interactions between particles in a degenerate quantum fluid has opened up a wide range of experiments in atomic and condensed matter physics. These include the creation of ultracold molecules<sup>1</sup>, investigation of the BEC-BCS cross-over regime<sup>2</sup>, and the enhancement of the sensitivity of an atom interferometer beyond the standard shot noise limit via squeezing<sup>3</sup>. The majority of these experiments use a Feshbach resonance, a magnetically-tunable molecular bound state, to vary the elastic scattering properties of a Bose-Einstein condensate. Only a few bosonic atoms have experimentally accessible Feshbach resonances. <sup>85</sup>Rb was the first such species to be condensed by the group of Cornell and Wieman in 2000<sup>4</sup>.

Here we describe our experimental setup for creating stable Bose-Einstein condensates of <sup>85</sup>Rb with tunable interparticle interactions, following the work of Papp *et. al.*<sup>5</sup>. Sympathetic cooling with <sup>87</sup>Rb cools the <sup>85</sup>Rb to quantum degeneracy in two stages, initially in a tight Ioffe-Pritchard magnetic trap and subsequently in a weak, large-volume crossed optical dipole trap. We use the 155 G Feshbach resonance to manipulate the elastic and inelastic scattering properties of the <sup>85</sup>Rb atoms. Typical condensates contain  $4 \times 10^4$  atoms with a scattering length of  $a = +200a_0$ . Our minimalist apparatus is well-suited to experiments on dual-species and spinor Rb condensates, and has several simplifications over the <sup>85</sup>Rb BEC machine at JILA.

---

<sup>1</sup>C.A. Regal, C. Ticknor, J.L. Bohn and D.S. Jin, *Nature* **424**, 47 (2003)

<sup>2</sup>M. Bartenstein, A. Altmeyer, S. Riedl, *et. al.*, *Phys. Rev. Lett.* **92** 203201 (2004)

<sup>3</sup>C. Gross, T. Zibold, E. Nicklas, J. Estève and M.K. Oberthaler, *Nature* **464**, 1165 (2010)

<sup>4</sup>S.L. Cornish, N.R. Claussen, J.L. Roberts, *et. al.*, *Phys. Rev. Lett.* **85**, 1795 (2000)

<sup>5</sup>S. Papp and C. Wieman, *Phys. Rev. Lett.* **97**, 180404 (2006)

# Finite temperature theory for novel cold gas systems

D. Baillie, P. B. Blakie, A. S. Bradley

*Jack Dodd Centre for Quantum Technology, Department of Physics,  
University of Otago, Dunedin, New Zealand.*

The phenomenal recent progress with the control of the external degrees of freedom of ultra-cold gases, and the advent of new species with long range interactions presents a range of new and exciting systems for exploring manybody physics. The meanfield description of these systems is challenging and demands the development of new systematic theoretical approaches that lead to tractable and accurate numerical schemes.<sup>1</sup> In this work we present a range of applications of finite temperature meanfield theory to such systems including:

**Bosons in optical lattices:** We develop a practical finite temperature theory for the superfluid regime of a Bose gas in an optical lattice with additional harmonic confinement. We derive an extended Bose-Hubbard model that is valid for shallow lattices and when excited bands are occupied. Using the Hartree-Fock-Bogoliubov-Popov (HFBP) meanfield approach, and applying local density and coarse-grained envelope approximations, we arrive at a theory that can be numerically implemented accurately and efficiently.<sup>2</sup> We also present theory for the critical temperature of a Bose gas in a combined harmonic lattice potential based on our theory. We develop practical expressions for the ideal-gas critical temperature, and corrections due to interactions, the finite-size effect, and occupation of excited bands.<sup>3</sup>

**Bosons or fermions in toroidal traps:** A scalable toroidal geometry presents an opportunity for creating large scale persistent currents in Bose-Einstein condensates, for studies of the Kibble-Zurek mechanism, and for investigations of toroidally trapped degenerate Fermi gases. We analytically and numerically consider the heating involved in isentropic loading of a HFBP Bose or spin-polarized Fermi gas from a harmonic trap into the *scale invariant* toroidal regime.<sup>4</sup>

**Fermions with dipolar interactions:** We develop a meanfield treatment of a trapped Fermi gas with dipolar interactions, based on self-consistent semiclassical Hartree-Fock theory that accounts for direct and exchange interactions. We present results for thermodynamic properties of the system and consider the effect that dipole-dipole interactions have on coherence.<sup>5</sup>

---

<sup>1</sup>D. Baillie, D., “Efficient numerical and analytical results for Bose and Fermi gases using the trap density of states”, in preparation

<sup>2</sup>D. Baillie and P. B. Blakie, “Finite-temperature theory of superfluid bosons in optical lattices”, Phys. Rev. A **80**, 033620 (2009)

<sup>3</sup>D. Baillie and P. B. Blakie, “Critical temperature of a Bose gas in an optical lattice”, Phys. Rev. A **80**, 031603(R) (2009)

<sup>4</sup>D. Baillie, P. B. Blakie and A. S. Bradley, “Geometric scale invariance as a route to macroscopic degeneracy: loading a toroidal trap with a Bose or Fermi gas”, arXiv:1005.0473

<sup>5</sup>D. Baillie and P. B. Blakie, “Thermodynamics and coherence of a trapped dipolar Fermi gas”, in preparation

# Dynamic Effects of a Feshbach Resonance on Bragg Scattering from a BEC

C. E. Sahlberg, R. J. Ballagh, C. W. Gardiner

*Jack Dodd Centre for Quantum Technology, Department of Physics, University of Otago, Dunedin, New Zealand*

It is possible to dramatically alter the inter-atomic interaction strength of a Bose-Einstein condensate (BEC) by tuning an external magnetic field in the vicinity of a magnetic Feshbach resonance, and to partially convert atomic condensates into molecular condensates<sup>1</sup>. In a recent experiment<sup>2</sup> Bragg spectroscopy has been used to probe the behaviour of a strongly interacting BEC of <sup>85</sup>Rb, near the wide Feshbach resonance at 155 G. Close to the resonance, the resulting Bragg spectra from this experiment show a significant deviation from any available theoretical predictions.

We present a theoretical model for Bragg scattering from a BEC in the vicinity of a magnetic Feshbach resonance, using a C-field formalism<sup>3</sup>. We model the Feshbach resonance by explicitly including the formation of bound pairs close to resonance, corresponding to an added molecular field in our formalism<sup>4</sup>. The binding energy of the molecules can be tuned to model resonance behaviour and the associated increase in the s-wave scattering length.

Numerical simulations based on this model show that the bound state of the resonance can play an important role in the dynamics of the condensate, but that the size of this effect is dependent on the properties of the Feshbach resonance in question.<sup>5</sup>

---

<sup>1</sup>E. A. Donley *et al.*, Nature (London) 417 (2002)

<sup>2</sup>S. B. Papp *et al.*, Phys. Rev. Lett. 101 (2008)

<sup>3</sup>P. B. Blakie *et al.*, Advances in Physics 57 (2008)

<sup>4</sup>E. Timmermans *et al.*, Phys. Rep. 315 (1999)

<sup>5</sup>C. E. Sahlberg *et al.*, in preparation

## Crossover from hydrodynamic to Josephson oscillations in a double well BEC

A.B. Bardón<sup>1</sup>, L.J. LeBlanc<sup>1</sup>, J. McKeever<sup>1</sup>, M.H.T. Extavour<sup>1</sup>, F. Piazza<sup>2</sup>, A. Smerzi<sup>2</sup>  
J.H. Thywissen<sup>1</sup>

<sup>1</sup>*Department of Physics, University of Toronto, Toronto, Ontario, Canada M5S 1A7*

<sup>2</sup>*CNR-INFN BEC center and Dipartimento di Fisica, Università di Trento, I-38050 Povo, Italy*

We create a superfluid weak link by placing a Bose Einstein condensate (BEC) in a double well potential. The Josephson junction analogue occurs when the barrier between the two wells is higher than the chemical potential of the condensate. This creates two superfluids that are connected only by tunneling through the barrier. The theory most often used to describe this system is a two-mode model, valid only for small tunneling parameter, which predicts phenomena such as plasma oscillations and the ac Josephson effect. Decreasing the barrier creates a bridge between the superfluids, allowing flow over the barrier. We measure the population in each well evolve after an initial population imbalance. Notably, in the low barrier regime, we see two frequencies in the population dynamics. If the initial imbalance is sufficiently high we observe macroscopic quantum self-trapping even when the barrier is lower than the chemical potential. A comparison of our data to a 3D GPE calculation suggests that the low-barrier collective modes of the BEC transform into the high-barrier modes: a low-energy inter-well plasma mode and the higher-energy intra-well collective modes.

# The Effects of Disorder on a Quasi-2D System of Ultra-Cold Atoms

M.C. Beeler, Matthew Reed, Tao Hong S.L. Rolston

*Joint Quantum Institute, University of Maryland, College Park, MD, United States*

An ultra-cold gas of atoms can be used to create many different model Hamiltonians. When tightly confined in one spatial dimension, the gas can become effectively two-dimensional. At low temperature, a quasi-2D Bose gas undergoes a Berezinskii-Kosterlitz-Thouless phase transition to a superfluid, mediated by the binding and unbinding of vortex pairs. As disorder affects vortex transport properties, a slight amount of fine-grain disorder in the potential energy may alter the properties of this phase transition. We will present progress towards experimental observations of a 2D Bose gas of rubidium atoms in the presence of disorder created by a laser speckle field.

# Particle Velocimetry of Bose-Einstein Condensates for Studies of Quantum Turbulence

C. Billington, S. Johnstone, K. Helmerson

*School of Physics, Monash University, Victoria 3800, Australia*

We simulate two species Bose-Einstein condensates in two dimensions. When one component supports quantised vortices, we show that it is possible for atoms of the other species to become trapped within the effective potential wells formed by the vortex cores. We aim to use this phenomenon to image vortex lines by fluorescence imaging of the trapped, “tracer particles”. The ability to image vortex lines in situ represents a technical breakthrough that will open up new avenues of investigation. In particular, it will allow the investigation of vortex dynamics, which govern much of the behaviour in quantum turbulence.

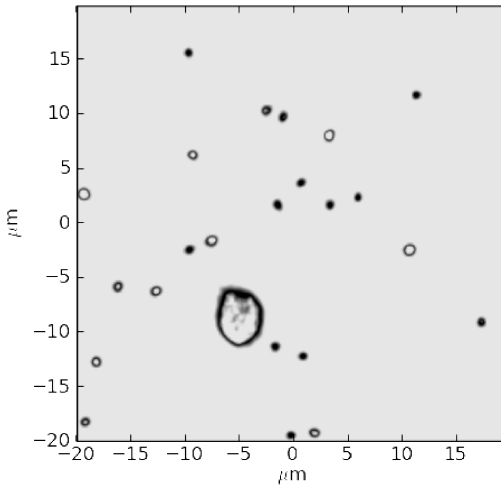


Figure 1: *The results of a simulation in which a  $^{23}\text{Na}$  BEC is stirred by a repulsive Gaussian potential, which a second component, of  $^{87}\text{Rb}$ , does not see. At  $t = 0$  all the rubidium resides within the region of low sodium density caused by the potential. The moving potential then acts as a bluff body and sheds vortices, in which rubidium atoms may become trapped. Lighter regions indicate higher atom density. This simulation has periodic boundary conditions and no trapping potential.*

# Finite temperature theory for the dipolar Bose gas

P.B. Blakie

*Jack Dodd Centre for Quantum Technology, Department of Physics, University of Otago, Dunedin, New Zealand.*

Ultra-cold gases with dipolar interactions are emerging as an exciting new system for exploring condensed matter physics. The long-range anisotropic nature of the dipolar interaction has made the theoretical description of the finite temperature regime difficult. In particular, in Bogoliubov treatments it has not been practical to include exchange interaction effects for the thermal fraction of the system<sup>1</sup>.

In this work we develop a new theoretical formalism for describing the equilibrium and nonequilibrium properties of a Bose gas with dipolar interactions. Our approach, based on the PGPE formalism<sup>2</sup>, includes direct and exchange interactions, and is applicable to the critical regime.

The system evolution is given by the dipolar PGPE:

$$i\hbar \frac{\partial \psi_{\mathbf{C}}}{\partial t} = H_0 \psi_{\mathbf{C}} + \mathcal{P}_{\mathbf{C}} \left\{ C_{\text{SR}} |\psi_{\mathbf{C}}(\mathbf{x})|^2 \psi_{\mathbf{C}}(\mathbf{x}) + D \int d^3x' \frac{1 - 3 \cos^2 \theta}{|\mathbf{x} - \mathbf{x}'|^3} |\psi_{\mathbf{C}}(\mathbf{x}')|^2 \psi_{\mathbf{C}}(\mathbf{x}) \right\},$$

where  $H_0$  is the single particle potential, including a harmonic trap,  $C_{\text{SR}}$  and  $D$  are the strengths of the short-range (van der Waals) and long-range (dipolar) interactions, respectively,  $\mathcal{P}_{\mathbf{C}}\{\}$  projects the evolution onto the region of highly occupied (classical) modes, and  $\theta$  is the angle between  $\mathbf{x}$  and the  $z$  axis (the axis along which the dipoles are polarized).

We have developed new numerical techniques to solve this equation<sup>3</sup> and are currently exploring the physics of this system at finite temperature. We present results for equilibrium properties near the transition point.

---

<sup>1</sup>Dipolar Bose-Einstein Condensates at Finite Temperature, S. Ronen and J. L. Bohn, Phys. Rev. A, **76** 043607 (2007)

<sup>2</sup>Dynamics and statistical mechanics of ultra-cold Bose gases using c-field techniques, P.B. Blakie, A.S. Bradley, M.J. Davis, R.J. Ballagh, and C.W. Gardiner, Adv. in Phys., **57**, 363 (2008)

<sup>3</sup>Numerical method for evolving the dipolar projected Gross-Pitaevskii equation, P. B. Blakie, C. Ticknor, A. S. Bradley, A. M. Martin, M. J. Davis, and Y. Kawaguchi, Phys. Rev. E **80**, 016703 (2009)

# Relative number squeezing in four wave mixing of matter waves

D. Boiron<sup>1</sup>, J.-C. Jaskula<sup>1</sup>, M. Bonneau<sup>1</sup>, V. Krachmalnicoff<sup>1</sup>, G. B. Partridge<sup>1</sup>,  
A. Aspect<sup>1</sup>, C. I. Westbrook<sup>1</sup>, K. V. Kheruntsyan<sup>2</sup>, P. Deuar<sup>3</sup>,

<sup>1</sup>Laboratoire Charles Fabry de l'Institut d'Optique, CNRS, Univ Paris-sud, Palaiseau, France

<sup>2</sup>Institute of Physics, Polish Academy of Sciences, Warsaw, Poland

<sup>3</sup>ARC Centre of Excellence for Quantum-Atom Optics, University of Queensland, Brisbane, Australia

The scattered atomic field resulting from the collision of two Bose-Einstein condensates of metastable helium is studied through a 3D single atom detector. To first order, the particles are scattered by pairs into a spherical halo of diameter the relative velocity between the 2 BECs. This atomic source should have similar quantum properties as the parametric down conversion source widely used in quantum optics. We have already demonstrated that particles of opposite and collinear velocities are correlated<sup>1</sup>.

We will present here the observation of relative number squeezing in such an experiment. We divide the scattering halo (excluding the BECs region) in  $4p$  slices and measure for each pair of slices  $(i, j)$  the atom number difference  $N_i - N_j$ . We then calculate its variance  $V_{i,j}$  averaging over 3600 shots. The variance should be Poissonian,  $V_{i,j} = \langle N_i + N_j \rangle$ , for uncorrelated pairs and sub-Poissonian for correlated ones. Fig. 1(a) gives the results of such a procedure for  $p = 4$ . We clearly see a squeezing for the 8 correlated pairs and no squeezing for the 112 uncorrelated ones. The amount of squeezing is largely limited by the finite detection yield ( $\sim 13\%$ ). It is also limited, to a smaller degree, by the finite width of the two-body correlation function of atoms of opposite velocities, which could induce a detection of atoms in a “wrong” slice. This effect should increase with the number of slices as observed and shown on Fig. 1(b).

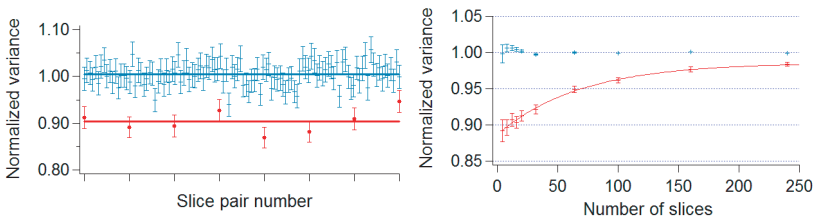


Figure 1: (a) Normalized variance  $V_{i,j}/\langle N_i + N_j \rangle$  of all pairs of slices  $(i, j)$ . The scattering halo has been divided in  $4p = 16$  slices. The normalized variance for the 8 correlated slice pairs has an average value of 0.904(8) whereas it is 1.005(2) for the uncorrelated ones. (b) Normalized variance in function of the number of slices.

<sup>1</sup>A. Perrin, H. Chang, V. Krachmalnicoff, M. Schellekens, D. Boiron, A. Aspect, C. I. Westbrook, Phys. Rev. Lett. **99**, 150405 (2007).

# Observation of vortex dipoles in an oblate Bose-Einstein condensate

T. W. Neely<sup>1</sup>, C. E. Samson<sup>1</sup>, A. S. Bradley<sup>2</sup>, M. J. Davis<sup>3</sup>, B. P. Anderson<sup>1</sup>

<sup>1</sup>College of Optical Sciences, University of Arizona, Tucson, Arizona 85721, USA

<sup>2</sup>Jack Dodd Centre for Quantum Technology, Department of Physics, University of Otago, Post Office Box 56, Dunedin, New Zealand

<sup>3</sup>The University of Queensland, School of Mathematics and Physics, ARC Centre of Excellence for Quantum-Atom Optics, Queensland 4072, Australia

A vortex dipole in a classical or quantum fluid consists of a pair of vortices of opposite circulation, with the dynamics of each vortex core dominated by the fluid flow pattern of the oppositely charged vortex and by the boundary conditions of the fluid. Although single vortices carry angular momentum, vortex dipoles can be considered as basic topological structures that carry linear momentum<sup>1</sup> in stratified or two-dimensional fluids. We report experimental observations and numerical simulations of the formation, dynamics, and lifetimes of single and multiply charged quantized vortex dipoles in highly oblate dilute-gas Bose-Einstein condensates (BECs).<sup>2</sup> We nucleate pairs of vortices of opposite charge (vortex dipoles) by forcing superfluid flow around a repulsive Gaussian obstacle within the BEC. By controlling the flow velocity we determine the critical velocity for the nucleation of a single vortex dipole, with excellent agreement between experimental and numerical results.

We present measurements of vortex dipole dynamics, as shown in Figure 1, finding that the vortex cores of opposite charge can exist for many seconds and that annihilation is inhibited in our trap geometry. For sufficiently rapid flow velocities, the experimental data suggests that clusters of like-charge vortices aggregate into long-lived multiply charged dipolar flow structures, and this behavior is confirmed by numerical simulations.

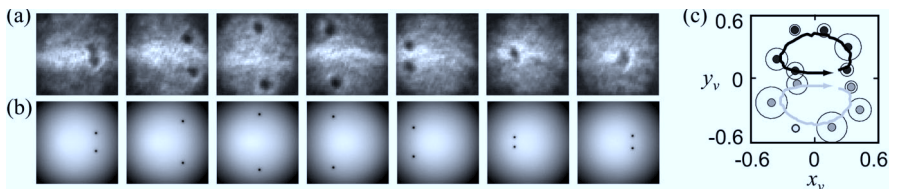


Figure 1: *Vortex dipole dynamics: (a) Experimentally observed atomic column density, imaged after the dipole is formed [destructive imaging at 200ms intervals]. (b) Numerical solution of the Gross-Pitaevskii equation. (c) Comparison of numerical vortex trajectories with data points averaged over several experimental runs<sup>1</sup>.*

<sup>1</sup>S. I. Voropayev and Y. D. Afanasyev, “Vortex Structures in a Stratified Fluid”, (Chapman and Hall, London, 1994).

<sup>2</sup>T. W. Neely, E. C. Samson, A. S. Bradley, M. J. Davis, and B. P. Anderson, “Observation of vortex dipoles in an oblate Bose-Einstein condensate”, Phys. Rev. Lett. **104**, 160401 (2010).

## Vortex Lattices in Anisotropic Traps

N. Lo Gullo<sup>1</sup>, S. McEndoo<sup>1</sup>, M. Paternostro<sup>2</sup> and Th. Busch<sup>1</sup>

<sup>1</sup>*Department of Physics, University College Cork, Cork, Republic of Ireland*

<sup>2</sup>*School of Mathematics and Physics, Queen's University Belfast, Belfast BT7 1NN, United Kingdom*

Vortices are topological excitations, which can be observed in rotating, superfluid Bose-Einstein condensates. Due to the single-valuedness condition of the wavefunction they can only carry quantised angular momentum and due to an energetic instability vortices with higher values of angular momentum decay into several vortices with winding number one. These vortices, in turn, arrange themselves into a well ordered lattice structure within the condensate and many beautiful experiments on these structures have been carried out in the recent decade.

The spatial distribution of the vortices in a rotating Bose-Einstein condensate is known to depend on the strength and shape of the external trapping potential. While for small anisotropies triangular lattices are still the energetically most favourable geometry, strongly anisotropic traps can lead to dramatic deviations from this way of patterning. Here we theoretically explore the lattice structure for the full range of anisotropies and medium rotation speeds. We show that the lattice structure undergoes a rich variety of structural changes, including the formation of stable zig-zag and linear configurations. Each of these spatial re-arrangements can be interpreted in terms of flow patterns in the background gas and is clearly signaled by a change in the behavior of the vortex-lattice eigenmodes.

This new degree of freedom gives a handle to study vortex behaviour and vortex-vortex interactions without being limited to the Abrikosov geometry. Furthermore, the topological nature of the vortices makes our findings applicable to systems beyond atomic Bose-Einstein condensates.

# Ion-induced Density Bubble in a Strongly Correlated One-dimensional Quantum Gas

J. Goold<sup>1,2</sup>, H. Doerk<sup>3</sup>, Z. Idziaszek<sup>4</sup>, T. Calarco<sup>5</sup> and Th. Busch<sup>1</sup>

<sup>1</sup>*Department of Physics, University College Cork, Cork, Republic of Ireland*

<sup>2</sup>*Centre for Quantum Technologies, National University of Singapore, 3 Science Drive 2, 117543, Singapore*

<sup>3</sup>*Max-Planck-Institut für Plasmaphysik, Boltzmannstr. 3, D-85748 Garching, Germany*

<sup>4</sup>*Institute of Theoretical Physics, Faculty of Physics, University of Warsaw, Hoza 69, PL-00681 Warsaw, Poland*

<sup>5</sup>*Institute for Quantum Information Processing, University of Ulm, Albert-Einstein-Allee 11, D-89069 Ulm, Germany*

Ultracold atom-ion hybrid systems are newly experimentally available systems which offer a large number of controls to explore new regimes of quantum mechanics in great detail. This is due to the polarisation potential of the ion as well as the possibility to move ions and atoms independently with respect to each other.

Here we consider a harmonically trapped Tonks-Girardeau gas of impenetrable bosons which is overlapping with a single embedded ion. The ion's charge induces an electric dipole moment in the atoms during a scattering process, which leads to an attractive  $r^{-4}$  potential for larger distances. At short range, however, the interaction is repulsive and can be modelled using quantum defect theory. We calculate the density profile of the gas in the presence of the ion located in the centre of the trap, using two realistic conditions: since the ion's trapping potential is usually several orders of magnitude larger than the atomic one, we treat the ion as a static deformation of the harmonic trap potential. Furthermore, due to the lack of possible relaxation processes in the Tonks-Girardeau regime we assume that the molecular bound states of the ionic potential are not populated. From this we derive the surprising finding that the presence of the ionic impurity leads to a density bubble in the gas of the order of  $1 \mu\text{m}$  for typical experimental parameters.

Furthermore, we show from these exact results that certain aspects of an ionic impurity in a Tonks gas can be described using a pseudopotential approximation for the interaction between the atoms and the ion, which allows for significantly easier treatment.

# Controlled Vortex Formation in an All-Optical Bose-Einstein Condensate

J.S. Butcher, L. Humbert, E.D. van Ooijen, S.A. Haine, N.R. Heckenberg,  
H. Rubinsztein-Dunlop

*University of Queensland, St Lucia, Queensland, Australia*

We are currently building an all-optical BEC and have designed a scanning beam trap that will trap atoms in a time averaged potential<sup>1</sup>. We plan to implement a new method of vortex creation which begins by loading the BEC into the scanning beam trap. The atoms are confined by a sheet of light and the focus of the scanning laser (waist= $4.5\mu\text{m}$ ). By gradually scanning away from the centre of the BEC using a 2D Acousto-Optic Modulator, the BEC is separated into four BECs. The scanning beam rapidly scans between the four spots at a rate fast enough for the atoms to remain trapped. The atoms are now essentially trapped in a quadruple well potential.

At this stage the power of the scanning beam at the four points changes, trapping the four BECs in four slightly different dipole potentials. This changes the rate at which the BECs evolve, imprinting a different phase change on each one. By carefully choosing the laser powers and the time for which they are increased/decreased, a  $2\pi$  phase loop can be engineered over the four BECs. When the four BECs are brought back together again, the  $2\pi$  phase loop creates a vortex in the final BEC.

We have successfully modeled this vortex creation method using the Gross-Pitaevskii equation and have chosen parameters that meet technical requirements. The required scanning sequence (splitting, phase imprinting and recombining) has been programmed and demonstrated using light. The optics for the scanning beam trap are now being aligned. Once the building of the all-optical BEC is complete, atoms will be loaded into the scanning beam trap to begin the experiment.

---

<sup>1</sup>S. K. Schnelle, E. D. van Ooijen, M. J. Davis, N. R. Heckenberg, and H. Rubinsztein-Dunlop. Versatile two-dimensional potentials for ultra-cold atoms. *Optics Express*, 16(3):14051412, 2008

# Matter wave amplification in a spatially modulated Bose gas released from an optical lattice

Xuzong Chen, Bo Lu, Thibault Vogt, Xinxing Liu, Xu Xu, Xuguang Yue, Xiaoji Zhou

*School of Electronics Engineering and Computer Science, Peking University, Beijing 100871, China*

Followed by our theoretical work <sup>1</sup>, the superradiance of a Bose gas released from an optical lattice was demonstrated for an angular condition of resonant diffraction by an off resonant laser pulse <sup>2</sup>. A Bose-Einstein condensate of  $2 \times 10^5$  <sup>87</sup>Rb atoms is loaded adiabatically along its long axis into an optical lattice formed with a retro-reflected laser beam ( $\lambda_L = 852\text{nm}$ ), focused on the BEC to a waist of  $110 \mu\text{m}$ . After holding a duration of 50 ms (Fig. 1(left)), we suddenly release the combined optical and magnetic traps. Following a delay  $\Delta t$ , a light pulse, red or blue detuned from the  $D_2$  transition ( $\lambda_S = 780 \text{ nm}$ ) by 1.3 GHz, is shined on the released matter waves.

As shown in Fig. 1(right), when the condensate is illuminated by a laser pulse when condensate released from a magnetic trap without lattice, we see normal superradiance pattern; however, when condensate is released from a lattice, we found the suppression of superradiance and matter wave amplification is observed. The compete between the superradiance and matter wave amplification is analyzed. Furthermore, we demonstrated the possibility of using matter wave amplification for characterizing spatial correlations of a Bose gas loaded in an optical lattice.

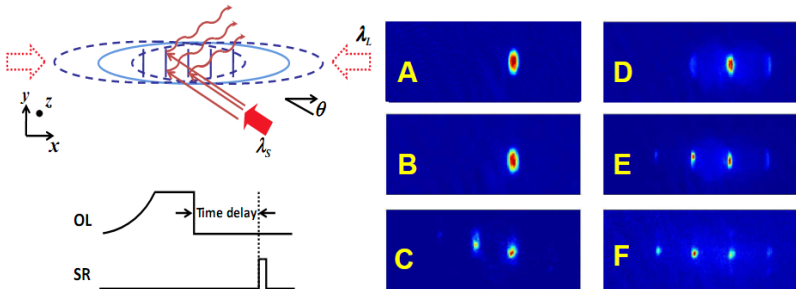


Figure 1: (left) Time sequential of the experiments. (right)(A) BEC. (B) and (C): BEC illuminated with a single off-resonant  $5 \mu\text{s}$  and  $40 \mu\text{s}$  laser pulse, respectively. (D) Atoms were released from an optical lattice potential with a potential depth of  $11E_r$ . (E) and (F): Matter wave amplification with  $5 \mu\text{s}$  and  $40 \mu\text{s}$  pulse after loading into an optical lattice ( $11E_r$  depth), respectively.

<sup>1</sup>Xu Xu, Xiaoji Zhou and Xuzong Chen, Phys. Rev. A **79**, 033605 (2009).

<sup>2</sup>Bo Lu, Thibault Vogt, Xinxing Liu, Xu Xu, Xuguang Yue, Xiaoji Zhou and Xuzong Chen, prepared.

# Atom Laser Locking, Four Wave Mixing and Single Mode Guiding with Metastable Helium Atoms

R.G. Dall, L.J. Byron, S.S. Hodgman, M.T. Johnsson, G.R. Dennis, J.J. Hope,  
K.G.H. Baldwin, A.G. Truscott

*Research School of Physics and Engineering, Australian National University,  
Canberra, ACT 0200, Australia*

In a metastable helium ( $\text{He}^*$ ) atom laser the constituent atoms have an enormous 20 eV of internal energy. This large internal energy makes high resolution measurements of the atom laser beam, using electronic detectors, straight-forward. Furthermore, when the atom laser beam is created Penning ionization occurs which leads to the production of ions. We have used these unique properties of a  $\text{He}^*$  atom laser beam to

(i) demonstrate locking of the atom laser beam: The ion signal produced when atoms are coupled out of a metastable helium Bose-Einstein condensate is used to actively lock the spatial location inside the condensate where outcoupling takes place. In doing so we remove unwanted amplitude, frequency, and spatial fluctuations from the output mode of the atom laser <sup>1</sup>.

(ii) create paired atom laser beams from a metastable helium atom laser via four-wave mixing. Radio frequency outcoupling is used to extract atoms from a Bose Einstein condensate near the center of the condensate and initiate scattering between trapped and untrapped atoms. The unequal strengths of the interactions for different internal states allows an energy-momentum resonance which leads to the creation of pairs of atoms scattered from the zero-velocity condensate. The resulting scattered beams are well separated from the main atom laser in the 2-dimensional transverse atom laser profile. Numerical simulations of the system are in good agreement with the observed atom laser spatial profiles, and indicate that the scattered beams are generated by a four-wave mixing process, suggesting that the beams are correlated <sup>2</sup>.

(iii) directly image, for the first time, the transverse mode structure of guided matter waves by taking advantage of the high detection efficiency which is characteristic of metastable helium ( $\text{He}^*$ ) atoms. We are able to observe end-on to the guiding structure the transverse spatial profile of the atoms as they strike our detector, thereby allowing direct measurement of the guided matter wave mode structure <sup>3</sup>.

---

<sup>1</sup>R.G. Dall, C.J. Dedman and A.G. Truscott. "Feedback control of an atom laser", *Optics Express* **16**, 14716 (2008).

<sup>2</sup>R.G. Dall, L.J. Byron, A.G. Truscott, G.R. Dennis, M.T. Johnsson and J.J. Hope. "Paired-atom laser beams created via four-wave mixing", *Physical Review A* **79**, 011601 (2009).

<sup>3</sup>R.G. Dall, S.S. Hodgman, M.T. Johnsson, K.G.H. Baldwin and A.G. Truscott. "Transverse mode imaging of guided matter waves", *Physical Review A* **81**, 011602 (2010).

# Theory of Two-Component BEC Interferometry

B.J. Dalton<sup>1</sup>, B.M. Garraway<sup>2</sup>

<sup>1</sup>*Swinburne University of Technology, Hawthorn, Victoria 3122, Australia*

<sup>2</sup>*University of Sussex, Falmer, Brighton BN1 9QH, UK*

Many previous treatments<sup>1,2</sup> for two component BEC interferometry are based on the simplest assumption that during the interferometric process the condensate is unfragmented, with all  $N$  bosons occupying the same single particle state. The latter is a linear superposition of two distinct single particle states (or modes),  $\phi_F(\mathbf{r},t) |F\rangle$  and  $\phi_G(\mathbf{r},t) |G\rangle$  that each boson could occupy - the internal states are  $|F\rangle, |G\rangle$ . The spatial wave functions  $\phi_a(\mathbf{r},t)$  ( $a = F, G$ ) satisfy coupled Gross-Pitaevskii equations. However, in more general two mode theories (both for two component<sup>3,4</sup> BECs and single component<sup>5,6,7</sup> BECs with orthogonal spatial modes), the quantum state is a superposition with amplitudes  $b_k(t)$  of Fock states with definite numbers  $\frac{N}{2} \mp k$  of bosons in the two modes ( $k = -\frac{N}{2}, \dots, \frac{N}{2}$ ), unfragmented states just being a special case. Fragmentation effects<sup>7</sup> (two single particle states having macroscopic occupancy) have been found. Spin angular momentum operators  $\hat{S}_\alpha$  ( $\alpha = x, y, z$ ) can be defined for two mode systems, the Bloch vector components are their expectation values in units of  $N$ .

By applying the Dirac-Frenkel variational principle we derive matrix mechanics equations for the amplitudes  $b_k(t)$  and generalized non-linear Gross-Pitaevskii equations for the mode functions  $\phi_a(\mathbf{r},t)$ . Self-consistent amplitude and mode equations are presented that are more general than expressions in<sup>1,2</sup>, and differ from those in<sup>3,4</sup>. Various BEC interferometry experiments, such as Ramsey interferometry can be treated. Collisions may be ignored during the short coupling pulses, where the evolution is equivalent to rotations of the Bloch vector. During the collision only evolution, the magnitudes of the amplitudes remain constant, but there is evolution of their phase factors. The Bloch vector undergoes Rabi oscillations and collision induced dephasing affects its  $x, y$  components.

If the spatial mode functions are assumed constant, the Hamiltonian can be described via the Josephson model, and a first approximation has been obtained for the amplitudes  $b_k(t)$ , enabling the evolution of the Bloch vector during the coupling  $\hat{H}_{Jos} \approx -J\hat{S}_x$  and collision stages  $\hat{H}_{Jos} \approx \delta\hat{S}_z + U\hat{S}_z^2$  to be determined. Spin squeezing effects are also studied. Here  $J$  is the time-dependent coupling parameter and  $\delta$  is the intercomponent transition energy. The collision parameter  $U$  may be enhanced by a large factor near a Feshbach resonance, increasing dephasing effects. All unfragmented states lie on the Bloch sphere of radius  $1/2$ , so if the Bloch vector leaves the Bloch sphere, fragmentation effects occur and the full generalised two mode theory would be required.

<sup>1</sup>P. B. Blakie, R. J. Ballagh and C. W. Gardiner, *J. Opt. B* 1, 378, 1999

<sup>2</sup>R. P. Anderson, C. Ticknor, A. I. Sidorov and B. V. Hall, *Phys. Rev. A* 80, 023603, 2009

<sup>3</sup>A. Sinatra and Y. Castin, *Eur. Phys. J. D* 8, 319, 2000

<sup>4</sup>Y. Li, P. Treutlein, J. Reichel and A. Sinatra, *Eur. Phys. J. B* 68, 365, 2009

<sup>5</sup>C. Menotti *et al*, *Phys. Rev. A* 63, 023601, 2001

<sup>6</sup>B. J. Dalton, *J. Mod. Opt.* 54, 615, 2007

<sup>7</sup>O. E. Alon *et al*, *Phys. Rev. A* 77, 033613, 2008

## Soliton creation during a Bose-Einstein condensation

B. Damski, W.H. Zurek

*Theoretical Division, Los Alamos National Laboratory, MS-B213, Los Alamos, NM  
87545, USA*

We use stochastic Gross-Pitaevskii equation to study dynamics of Bose-Einstein condensation. We show that cooling into a Bose-Einstein condensate can create solitons with density given by the cooling rate and by the critical exponents of the transition. Thus, counting solitons left in its wake should allow one to determine the critical exponents  $z$  and  $\nu$  for a thermal gas - Bose-Einstein condensate phase transition. The same information can be extracted from non-equilibrium two-point correlation functions.

Our results can be used for the experimental determination of these critical exponents. They also illustrate how universal dynamics of classical second order phase transitions can be studied with ultracold atoms.

This work was published in Phys. Rev. Lett. **104**, 160404 (2010). We acknowledge the support of the U.S. Department of Energy through the LANL/LDRD Program.

# Proposal to realise a Kibble-Zurek mechanism in a spin-1/2 Bose-Einstein condensate

J. Sabbatini, M.J. Davis

*The University of Queensland, School of Mathematics and Physics, ARC Centre of Excellence for Quantum-Atom Optics, Brisbane, Qld 4072, Australia*

The Kibble-Zurek mechanism is a universal theory for estimating the density of topological defects formed in both quantum and classical phase transitions. It has been applied to a wide range of systems covering classical and quantum physics, and from liquid crystals through to cosmological scenarios. The ideas were first developed by Kibble in cosmology to estimate the density of cosmic strings<sup>1</sup>, and successively extended by Zurek to quenches in condensed matter systems such as liquid helium<sup>2</sup>. Recently two pioneering experiments<sup>3,4</sup> have reported the observation of spontaneous formation of topological defects in Bose-Einstein condensates, opening a new arena for testing and understanding the microscopic physics of defect formation.

Here we propose realising a novel Kibble-Zurek mechanism in a coupled, two component Bose-Einstein condensate, as realised by trapping two hyperfine states of a single atomic species. These systems are characterised by the interspecies  $g_{12}$  and intraspecies  $g_{11}$  and  $g_{22}$  interaction constants. If  $\Delta = g_{11}g_{22} - g_{12}^2$  is negative the ground state of the system is phase segregated, as “unlike” atoms repel each other more strongly than “like” atoms. However, Merhasin *et al.* have shown that a linear coupling  $\Omega$  between the two components has the effect of lowering the effective interspecies scattering length<sup>5</sup>. With the coupling above a critical value  $\Omega > \Omega_{cr}$  a previously phase segregated system will become fully miscible.

A quantum Kibble-Zurek scenario is realised by beginning with an elongated two-component Bose-Einstein condensate with a coupling  $\Omega$  such that the system is in the miscible phase. The coupling  $\Omega$  is then dynamically reduced to zero resulting in spontaneous pattern formation. The density of the resulting domain walls depends crucially on the ramp rate. We numerically demonstrate the scaling law predicted by the Kibble-Zurek mechanism from the critical exponents of the system. The parameters required for realising this experiment and observing Kibble-Zurek scaling are currently attainable in many ultra-cold atom laboratories worldwide.

<sup>1</sup>T. W. B. Kibble, Topology of cosmic domains and strings, *Journal of Physics A* **9**, 1387, (1976).

<sup>2</sup>W. H. Zurek, Cosmological experiments in superfluid helium?, *Nature (London)* **317**, 505, (1985).

<sup>3</sup>L. E. Sadler, J. M. Higbie, S. R. Leslie, M. Vengalattore and D. M. Stamper-Kurn, Spontaneous symmetry breaking in a quenched ferromagnetic spinor Bose-Einstein condensate, *Nature (London)* **443**, 312, (2006).

<sup>4</sup>C. N. Weiler, T. W. Neely, D. R. Scherer, A. S. Bradley, M. J. Davis and B. P. Anderson, Spontaneous vortices in the formation of Bose-Einstein condensates, *Nature* **455**, 948, (2008).

<sup>5</sup>I. M. Merhasin, B. A. Malomed and R. Driben, Transition to miscibility in a binary Bose-Einstein condensate induced by linear coupling, *Journal of Physics B* **38**, 877, (2005).

# Generating Entangled Atom Lasers

G.R. Dennis<sup>1,2</sup>, M.T. Johansson<sup>1,2</sup>

<sup>1</sup>*Department of Quantum Science, Australian National University, Canberra, ACT, Australia*

<sup>2</sup>*ARC Centre of Excellence for Quantum Atom Optics, Australia*

We present a method to create paired atom laser beams from a metastable helium Bose-Einstein condensate via four-wave mixing, analogous to nondegenerate parametric down conversion in optical systems. The two atomic beams are entangled upon production, although the extent to which this entanglement survives on leaving the condensate is currently uncertain. Robust number difference squeezing between the beams is expected, however. The crucial part of the scheme relies on the BEC components having differing  $s$ -wave scattering lengths, suggesting that the scheme may work for other atomic species as well. We study this system through an extension of the usual Bogoliubov technique generalised to consider perturbations about a time-dependent, but periodic mean-field.

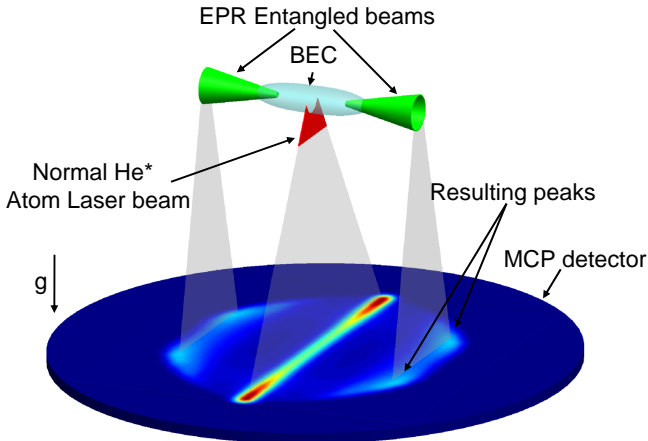


Figure 1: *Schematic of the experimental setup.*

# Superfluid Critical Velocity in Trapped Bose-Einstein Condensates

C. Feng, M.J. Davis

*ARC Centre of Excellence for Quantum Atom-Optics, University of Queensland,  
Brisbane, Queensland, 4072, Australia*

A defining feature of superfluidity is the presence of frictionless flow. In the archetypal case, a macroscopic impurity in the form of a repulsive laser beam is moved through a superfluid at various velocities and a sharp threshold or critical velocity is observed for the onset of excitations<sup>1,2</sup>. Landau's original analysis<sup>3</sup> for superfluid Helium when applied to dilute gas Bose-Einstein condensates (BECs), a class of superfluids, predicts a critical velocity based on phonon excitations equal to the speed of sound in the condensate. However, experiments and simulations show a critical velocity well below the mean system sound speed. Furthermore, common to existing numerical<sup>4,5</sup> and experimental<sup>1,2,6</sup> studies is the onset of soliton or vortex formation, which is not incorporated in the original Landau analysis. A complexity is that experiments to date have used atom trapping potentials that have resulted in inhomogeneous condensate profiles. Within the local density approximation (LDA), this results in a position-dependent coherence length and sound speed, such that the condensate has no single well-defined critical velocity.

In this work, we construct a phenomenological model for the energy transferred to a trapped condensate after one pass of a moving obstacle. We do this by evaluating the fractional volume of the condensate that falls above or below physically motivated thresholds for the onset or suppression of excitations. In effect, we treat the inhomogeneous condensate as composed of homogeneous subregions under the LDA where the form of the critical velocity is the same for all subregions but the precise value is a function of the local density. Our model is then compared to dynamical simulations of harmonically trapped BECs perturbed by a moving potential using the cylindrically symmetric 3D Gross Pitaevskii equation as well as to the experimental results in reference [1]. When applied to a homogeneous system, our results quantitatively describes the crucial role of soliton excitations in governing the excitation thresholds. Using this model, the Landau critical velocity for the homogeneous system can be determined from measurements in trapped condensates.

---

<sup>1</sup>P. Engels and C. Atherton, *Phys. Rev. Lett.*, **99** 160405, 2007.

<sup>2</sup>R. Onofrio, C. Raman, J.M. Vogels, J.R. Abo-Shaeer, A.P. Chikkatur and W. Ketterle, *Phys. Rev. Lett.*, **85** 2228 - 2231, 2000.

<sup>3</sup>I. M. Khalatnikov translated by P. C. Hohenberg, *An Introduction to the Theory of Superfluidity*, W. A. Benjamin Inc., 1965.

<sup>4</sup>V. Hakim, *Phys. Rev. E*, **55** 2835 - 2845, 1997

<sup>5</sup>N. Pavloff, *Phys. Rev. A*, **66** 013610, 2002.

<sup>6</sup>T.W. Neely, E.C. Samson, A.S. Bradley, M.J. Davis and B.P. Anderson, *Phys. Rev. Lett.*, **104** 160401, 2010.

# Midlands Ultracold Atom Research Centre at Nottingham, UK

T. Fernholz, L. Hacker Müller and P. Krüger

*Midlands Ultracold Atom Research Centre, School of Physics and Astronomy, The University of Nottingham, UK*

Recently the Midlands Ultracold Atom Research Centre (MUARC) was established following a joint initiative of the Universities of Nottingham and Birmingham. The research efforts at the Centre target questions at the interface of ultracold atom research, condensed matter physics, and quantum optics. Here we introduce the experimental programme at the Nottingham node of MUARC. We have begun to assemble three apparatus with different focus but at the same time substantial overlap. The status of design and construction will be discussed and the planned experiments will be outlined. The themes we envision to touch upon are:

- Atom-light interfaces and quantum memories
- Quantum degenerate Bose gases in low dimensions and non-trivial topologies (rings, cylinders, tori)
- Coherence of quantum gases in non-equilibrium and dynamical situations
- Atom-(semiconductor) surface interactions
- Bose-Fermi mixtures in low dimensions and near surfaces

The central tools to be employed in our experiments will be microengineered atom chips. We will present a number of technical aspects of our implementations and outline future development plans of chips, including the use of advanced materials such as structured semiconductors.

# Formation Dynamics of Non-Equilibrium Bose-Einstein Condensates

M.C. Garrett and M.J. Davis

*ARC Centre of Excellence for Quantum-Atom Optics, School of Mathematics and Physics, The University Queensland, Brisbane, QLD 4072, Australia*

The dynamics of phase transitions are important in a wide range of physical systems but can be difficult to study, both experimentally and theoretically. The Bose-Einstein condensation (BEC) phase transition is therefore of interest due to its experimental tunability and theoretical tractability. A number of experiments studying BEC formation dynamics have been well-described by kinetic theory, where the condensate mode grows in quasistatic equilibrium<sup>1,2,3</sup>. However, some other experiments have witnessed the formation of strongly nonequilibrium condensates, evidenced by the observation of shape oscillations<sup>4</sup>, vortices<sup>5</sup>, and solitons<sup>6</sup>.

To gain further theoretical insight into the formation of nonequilibrium BEC, we consider the importance of nonequilibrium dynamics in the thermal cloud. We begin with the stochastic Gross-Pitaevskii equation (SGPE) formalism<sup>7,8</sup>, in which the highly occupied, low-energy modes are described by a classical field equation, coupled to a reservoir (the thermal cloud) parametrized by temperature  $T(t)$  and chemical potential  $\mu(t)$ . In our present work, we aim to couple the SGPE to a nonequilibrium thermal cloud in the hydrodynamic regime, parametrized by position-dependent temperature  $T(\mathbf{r}, t)$  and chemical potential  $\mu(\mathbf{r}, t)$ . After calculating the initial values of these parameters based on rapid local thermalization following a sudden rf quenching, we will use hydrodynamic equations similar to those described by Zaremba, Griffin, and Nikuni<sup>9</sup> to simulate the dynamics of the thermal cloud within the effective potential created by the mean-field of the growing condensate.

<sup>1</sup>H.-J. Miesner, D. M. Stamper-Kurn, M. R. Andrews, D. S. Durfee, S. Inouye, and W. Ketterle, "Bosonic Stimulation in the Formation of a Bose-Einstein Condensate", *Science* **279**, 1005 (1998).

<sup>2</sup>M. Köhl, M. J. Davis, C. W. Gardiner, T. W. Hänsch, and T. Esslinger, "Growth of Bose-Einstein Condensates from Thermal Vapor", *Phys. Rev. Lett.* **88**, 080402 (2002).

<sup>3</sup>M. Hugbart, J. A. Retter, A. F. Varón, P. Bouyer, and A. Aspect, "Population and phase coherence during the growth of an elongated Bose-Einstein condensate", *Phys. Rev. A* **75**, 011602(R) (2007).

<sup>4</sup>I. Shvarchuck, Ch. Buggle, D. S. Petrov, K. Dieckmann, M. Zielonkowski, M. Kemmann, T. G. Tiecke, W. von Klitzing, G. V. Shlyapnikov, and J. T. M. Walraven, "Bose-Einstein Condensation into Nonequilibrium States Studied by Condensate Focusing", *Phys. Rev. Lett.* **89**, 270404 (2002).

<sup>5</sup>C. N. Weiler, T. W. Neely, D. R. Scherer, A. S. Bradley, M. J. Davis, and B. P. Anderson, "Spontaneous vortices in the formation of Bose-Einstein condensates", *Nature* **455**, 948 (2008).

<sup>6</sup>J. Chang, C. Hamner, and P. Engels, "Formation of Solitons During the BEC Phase Transition", *APS DAMOP* (2009).

<sup>7</sup>C. W. Gardiner and M. J. Davis, "The stochastic Gross-Pitaevskii equation: II", *J. Phys. B: At. Mol. Opt. Phys.* **36**, 4731 (2003).

<sup>8</sup>P. B. Blakie, A. S. Bradley, M. J. Davis, R. J. Ballagh, and C. W. Gardiner, "Dynamics and statistical mechanics of ultra-cold Bose gases using c-field techniques", *Adv. Phys.* **57**, 363 (2008).

<sup>9</sup>E. Zaremba, A. Griffin, and T. Nikuni, "Two-fluid hydrodynamics for a trapped weakly interacting Bose gas", *Phys. Rev. A* **57**, 4695 (1998).

# Formation of skyrmion lattice in a rapidly-quenched and fast-rotating ferromagnetic spinor Bose-Einstein condensate

S.-W. Su<sup>1</sup>, I.-G. Liu<sup>2</sup>, C.-H. Hsueh<sup>2</sup>, Y.-C. Tsai<sup>3</sup>, T.-L. Horng<sup>4</sup>, S.-C. Gou<sup>2</sup>

<sup>1</sup>*Department of Physics, National Tsing Hua University, Hsin Chu, Taiwan*

<sup>2</sup>*Department of Physics, National Chang Hua University of Education, Chang Hua, Taiwan*

<sup>3</sup>*Department of Photonics, Feng Chia University, Taichung, Taiwan*

<sup>4</sup>*Department of Applied Mathematics, Feng Chia University, Taichung, Taiwan*

We predict the formation of skyrmion lattice in a rapidly rotating ferromagnetic spinor Bose-Einstein condensate. The dynamics of an  $F = 1$  spinor Bose-Einstein condensate of  $^{87}\text{Na}$  during the rotating evaporative cooling is investigated by numerically solving the stochastic projected Gross-Pitaevskii equation. We show that, when the rotating cloud reaches equilibrium at very low temperatures, very three vortices in each condensate component would closely bind up and form a triplet. These vortex triplets arrange themselves into some repeated spatial structures but do not form vortex lattices. On the other hand, the local spin textures of the rotating spinor BEC do form lattice structures. Our numerical results suggest that when the system reaches thermal equilibrium, a triangular lattice of skyrmions with unit topological charge can be generated in the condensate. The dynamical stability of this lattice structure is examined.

# Coherent transfer of ultracold photoassociated molecules into the rovibrational ground state

K. Aikawa<sup>1</sup>, K. Oasa<sup>1</sup>, J. Kobayashi<sup>1</sup>, M. Ueda<sup>2,3</sup>, S. Inouye<sup>1,3</sup>

<sup>1</sup>*Department of Applied Physics, The University of Tokyo, Yayoi, Bunkyo-ku, Tokyo, Japan*

<sup>2</sup>*Department of Physics, The University of Tokyo, Hongo, Bunkyo-ku, Tokyo, Japan*

<sup>3</sup>*ERATO Macroscopic Quantum Control Project, JST, Yayoi, Bunkyo-ku, Tokyo, Japan*

Ultracold polar molecules offer a wide variety of new applications, ranging from novel quantum phases to quantum computation and precision measurement. Though photoassociation and magnetoassociation enable us to produce ultracold molecules in their high vibrational levels, it is crucially important to transfer them to the absolute ground state for those applications. Incoherent transfer methods demonstrated so far<sup>1,2,3</sup> populate multiple rotational levels. Stimulated Raman Adiabatic Passage (STIRAP) has been expected to be a powerful tool to populate a single level, but so far it has been demonstrated only for Feshbach molecules<sup>4,5</sup>.

Here we report on the SITRAP transfer of weakly bound <sup>41</sup>K<sup>87</sup>Rb molecules produced by photoassociation (PA) into the rovibrational singlet ground state. Starting from laser-cooled <sup>41</sup>K and <sup>87</sup>Rb atoms, molecules in the  $v = 90 - 94$  of  $X^1\Sigma^+$  and the  $v = 20 - 25$  of  $a^3\Sigma^+$  were produced. Among them, molecules in the  $v = 91$ ,  $N = 0$  of  $X^1\Sigma^+$  were transferred into the single rotational level  $v = 0$ ,  $N = 0$  of  $X^1\Sigma^+$  with the intermediate state of the  $v = 41$ ,  $N = 1$  of  $(3)^1\Sigma^+$ . The narrow natural linewidth of the intermediate state ( $\sim 300$ kHz) allows the successful transfer despite the small power ( $\sim 10$ mW) and the large beam diameter ( $\sim 1.5$ mm) of the Raman lasers. A transfer into the  $N = 2$  level was also demonstrated and the rotational constant was determined to be  $B = 1095.4(1)$  MHz, which was consistent with the value for <sup>40</sup>K<sup>87</sup>Rb<sup>6</sup>.

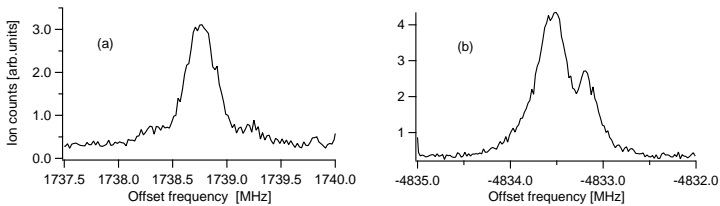


Figure 1: Spectrum of STIRAP transfer into the  $v = 0$ , (a)  $N = 0$  and (b)  $N = 2$  of the  $X^1\Sigma^+$  level. Produced molecules were directly detected by multiphoton ionization.

<sup>1</sup>J.M. Sage et al., Phys.Rev.Lett. **94**, 203001 (2005)

<sup>2</sup>M. Viteau et al., Science **321**, 232

<sup>3</sup>J. Deiglmayr et al., Phys.Rev.Lett. **101**, 133004 (2008)

<sup>4</sup>K.-K. Ni et al., Science **322**, 231 (2008)

<sup>5</sup>J.G. Danzl et al., Nature Physics **6**, 265 (2010)

<sup>6</sup>S. Ospelkaus et al., Phys.Rev.Lett. **104**, 030402 (2010)

# Dipolar relaxation of a chromium Bose-Einstein condensate in optical lattices

G. Bismut<sup>1,2</sup>, B. Pasquiou<sup>1,2</sup>, B. Laburthe-Tolra<sup>1,2</sup>, E. Maréchal<sup>1,2</sup>, P. Pedri<sup>1,2</sup>,  
L. Vernac<sup>1,2</sup> and O. Gorceix<sup>1,2</sup>,

<sup>1</sup>Université Paris 13, Laboratoire de Physique des Lasers, Institut Galilée, 99 Ave J.B. Clément, F-93430 Villetaneuse, France

<sup>2</sup>CNRS, UMR 7538, 99 Ave J.B. Clément, F-93430 Villetaneuse, France

Dipole-dipole interactions are long-ranged and anisotropic. They induce a coupling between spin and angular momentum degrees of freedom yielding new interesting physics in the field of dilute quantum gases. Specifically, we study dipolar relaxation (DR) processes in a chromium BEC<sup>1</sup> transferred into an excited magnetic sublevel and loaded in 1D and 2D optical lattices. This work which extends previous work<sup>2</sup> demonstrates and quantifies how the confinement of a quantum gas in optical lattices deeply modifies the DR processes. In particular, we show that DR is strongly inhibited at low magnetic fields when the released energy becomes smaller than the vibrational quantum of energy at the bottom of the lattice wells. This work is supported by the "Ministre de l'Enseignement Supérieur et de la Recherche" (within CPER) and by IFRAC.

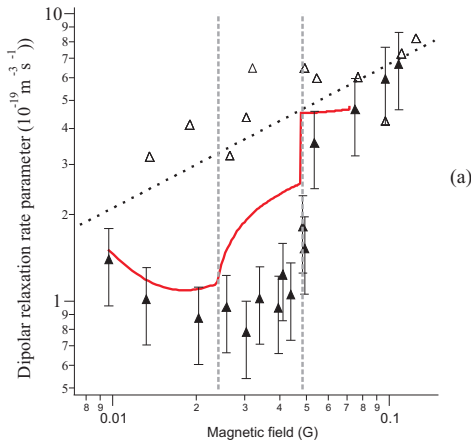


Figure 1: DR loss parameter vs  $B$ -field in a 1D lattice (full triangles) and in open space (open triangles). Dashed lines show the excitation thresholds in the lattice. The theoretical curves (below) are drawn for two orthogonal orientations of the field with respect to the 2D pancake planes.

<sup>1</sup>Q. Beaufils et al., Phys. Rev. A 77, 053413 (2008)

<sup>2</sup>B. Pasquiou et al., Phys. Rev. A 81, 042716 (2010)

# Dipolar effects on the excitation spectrum of a chromium Bose-Einstein condensate

G. Bismut<sup>1,2</sup>, B. Pasquiou<sup>1,2</sup>, B. Laburthe-Tolra<sup>1,2</sup>, E. Maréchal<sup>1,2</sup>, P. Pedri<sup>1,2</sup>,  
L. Vernac<sup>1,2</sup> and O. Gorceix<sup>1,2</sup>,

<sup>1</sup>Université Paris 13, Laboratoire de Physique des Lasers, Institut Galilée, 99 Ave J.B. Clément, F-93430 Villetaneuse, France

<sup>2</sup>CNRS, UMR 7538, 99 Ave J.B. Clément, F-93430 Villetaneuse, France

We report on the first experimental demonstration of the impact of dipole-dipole interactions on the collective excitations of a dilute quantum gas. We precisely measure the frequency of one of the quadrupolar vibration modes of a trapped chromium BEC<sup>1</sup>. The frequency of this mode is shifted when the orientation of the atom spin with respect to the trap axes is changed. The agreement with previous theoretical predictions<sup>2</sup> is excellent. Furthermore, comparison of our experimental outcomes with numerical simulations<sup>3</sup> sheds light on the range of validity of the Thomas-Fermi approach at limited atom numbers and demonstrates how the study of BEC excitations is a sensitive probe of dipolar interactions. This work is supported by the "Ministère de l'Enseignement Supérieur et de la Recherche" (within CPER) and by IFRAF.

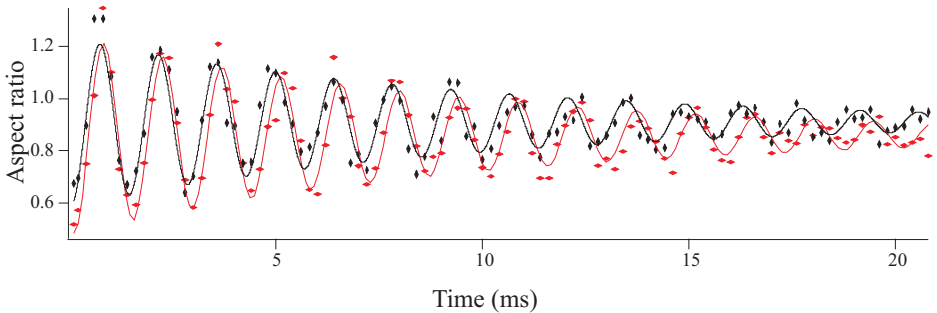


Figure 1: Influence of dipolar interaction on the intermediate quadrupole mode frequency. Free oscillations of the mode after an excitation is observed by measuring the aspect ratio of the BEC, given by the measurement of its two Thomas-Fermi radii along axes perpendicular to the imaging beam. The magnetic field is either vertical (black diamonds) or parallel to the horizontal imaging beam (red dots). We plot as well the best fits from damped sinusoidal forms.

<sup>1</sup>Q. Beaufils et al., Phys. Rev. A 77, 053413 (2008)

<sup>2</sup>D. O'Dell et al., Phys. Rev. Lett. 92, 250401 (2004)

<sup>3</sup>G. Bismut et al., submitted, arXiv:1005.2493

# Solids, Supersolids, and Pairing with Cold Polar Molecules

B. Capogrosso-Sansone

*Institute for Theoretical Atomic, Molecular and Optical Physics, Harvard-Smithsonian  
Center of Astrophysics, Cambridge, MA, 02138, USA*

We consider a mixture of hard core bosonic polar molecules, interacting via repulsive dipole-dipole interactions, and one atomic bosonic species confined on a two-dimensional square lattice. We study how the presence of atoms affects the robustness of molecular solid phases both at zero and finite temperature. We find that, due to atom-molecule attractive contact potential, solid phases can be stabilized at both, (much) lower strengths of dipolar interactions and higher temperatures. As a byproduct, atoms can also order in a solid phase with same melting temperatures as for molecules. We also find that for large enough attraction between atoms and molecules a paired supersolid phase is stabilized.

# Wigner Crystallization of Rotating Dipolar Fermions in the Fractional Quantum Hall Regime

Szu-Cheng Cheng<sup>1</sup>, Shih-Da Jheng<sup>2</sup>, T. F. Jiang<sup>2</sup>

<sup>1</sup>*Department of Physics, Chinese Culture University, Taipei 11114, Taiwan*

<sup>2</sup>*Institute of Physics, National Chiao Tung University, Hsinchu 30010, Taiwan*

We show the possible existence of a two-dimensional (2D) Wigner crystal (WC) in the Fractional Quantum Hall regime. We consider the effect of Landau-level mixing (LLM) by applying a variational wave function to obtain the ground-state energy of the WC. The strength of LLM is related to the LLM parameter  $\gamma = \nu r_s / 2\pi$ , where  $\nu$  and  $r_s$  are the filling factor of Landau levels and the dimensionless inverse distance of fermions, respectively. The large  $r_s$  value corresponds to the high density. There is a strong LLM in the fractional quantum Hall regime if  $r_s$  is big and  $\nu$  is fixed. We then find that the LLM will lower the energy of the WC significantly in the high-density regime. We conclude that The WC has a lower/higher energy than the quantum Hall liquid in the high-density/low-density regime (see Fig. 1), respectively. This conclusion is consistent with non-rotating dipolar gases<sup>1</sup>, but is inconsistent with the low-density conclusion from Baranov *et al.*<sup>2</sup>, where the effect of LLM is ignored.

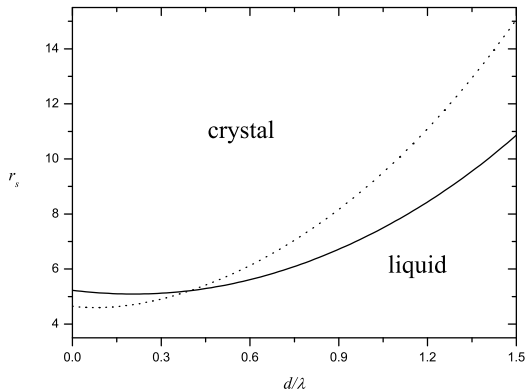


Figure 1: Phase diagram of rotating dipolar gases. The solid and dotted lines indicate the critical dimensionless length  $r_s$  as a function of the thickness  $d/\lambda$  for  $\nu=1/5$  and  $\nu=1/3$ , respectively. Here  $\lambda = \sqrt{\hbar/M\omega_z}$ , where  $M$  is the mass of a fermion and  $\omega_z$  is the trapping frequency in the direction that is perpendicular to the 2D plane.

<sup>1</sup>H. Büchler, E. Demler, M. Lukin, A. Micheli, N. Prokof'ev, G. Pupillo, and P. Zoller, "Strongly Correlated 2D Quantum Phases with Cold Polar Molecules: Controlling the Shape of the Interaction Potential.", Phys. Rev. Lett. **98**, 060404 (2007).

<sup>2</sup>M. Baranov, H. Fehrmann, and M. Lewenstein, "Wigner Crystallization in Rapidly Rotating 2D Dipolar Fermi Gases.", Phys. Rev. Lett. **100**, 200402 (2008).

## Exact multichannel calculations of 2s2p bound levels in bosonic and fermionic ultracold helium dimers

D. G. Cocks<sup>1</sup>, I. B. Whittingham<sup>1</sup>, G. Peach<sup>2</sup>

<sup>1</sup>*School of Engineering and Physical Sciences, James Cook University, Townsville, 4811, Australia*

<sup>2</sup>*Department of Physics and Astronomy, University College London, London, WC1E 6BT, UK*

Multichannel calculations<sup>1</sup> have been performed of molecular bound levels that include non-adiabatic and Coriolis couplings. These bound levels are accessible from gases of ultracold metastable helium by single-photon transitions to the 2s2p manifold. The bosonic form, helium-4, has been previously investigated theoretically via approximate single-channel calculations<sup>2</sup> and the current results show that important differences are present in the exact multichannel calculation. Furthermore, observability criteria have been formulated that allow an almost unique assignment of theoretical levels with experimental observations<sup>3,4,5</sup>. To reconcile small differences between theory and experience, a small 1% correction to the input Born-Oppenheimer potentials in the region of the inner classical turning point has been applied that significantly improves the results.

Preliminary results of the calculation extended to the fermionic helium-3 system are also presented. We compare our results to those of Dickinson<sup>6</sup> who performed calculations in the single-channel approximation. The hyperfine structure, which is absent in helium-4, is of a comparable magnitude to the fine-structure and causes a significant difference in behaviour in the calculations. The short-range correction, that was formulated in the helium-4 system, is applied to helium-3 and the differences in results analysed.

---

<sup>1</sup>D. G. Cocks, I. B. Whittingham and G. Peach, 2010 Submitted to *J. Phys. B*, arXiv:0911.0237

<sup>2</sup>B. Deguilhem, T. Leininger, F. X. Gadéa and A. S. Dickinson, 2009 *J. Phys. B* **42** 015102.

<sup>3</sup>J. Kim, U. D. Rapol, S. Moal, J. Léonard, M. Walhout and M. Leduc, 2004 *Eur. Phys. J. D* **31** 227-37.

<sup>4</sup>M. van Rijnbach, *Ph.D thesis* "Dynamical spectroscopy of transient He<sub>2</sub> molecules", 2004 University of Utrecht.

<sup>5</sup>P. J. J. Tol, *Ph.D thesis* "Trapping and evaporative cooling of metastable helium", 2005 Free University of Amsterdam.

<sup>6</sup>A. Dickinson, 2006 *Eur. Phys. J. D* **37** 435-9.

# Equilibrium Properties of Trapped Dipolar Gases at Finite Temperatures

Y Endo<sup>1</sup>, T. Miyakawa<sup>2</sup>, T. Nikuni<sup>1</sup>

<sup>1</sup>*Department of Physics, Tokyo University of Science, Tokyo, Japan*

<sup>2</sup>*Faculty of Education, Aichi University of Education, Aichi, Japan*

We study equilibrium properties of dipolar Fermi gases<sup>1</sup> and dipolar Bose gases at finite temperatures. We introduce a variational ansatz for the phase-space distribution function that can describe the deformation in both real space and momentum space<sup>2</sup>. The effect of different statistics on the dipolar interactions is discussed with particular emphasis on the deformation in momentum space. We examine the stability of the system by varying the temperature, trap aspect ratio and the dipole moment. In addition, we discuss how the deformation in both real space and momentum space can be observed in the high-temperature regime, which is relevant to the current experiments at JILA [K. K. Ni et. al. *Science* 322, 231 (2008)<sup>3</sup>] and at Tokyo univ. [K. Aikawa et. al. *New J. Phys.* 11, 055035 (2009)<sup>4</sup>]

---

<sup>1</sup>Y. Endo, T. Miyakawa and T. Nikuni, arXiv: 1002. 0408 (2010).

<sup>2</sup>T. Miyakawa, T. Sogo, and H. Pu, *Phys. Rev. A* 77, 061603(R) (2008).

<sup>3</sup>K. K. Ni, S. Ospelkaus, M. H. G. de Miranda, A. Peer, B. Neyenhuis, J. J. Zirbel, S. Kotochigova, P. S. Julienne, D. S. Jin, and J. Ye, *Science* 322, 231 (2008).

<sup>4</sup>K. Aikawa, D. Akamatsu, J. Kobayashi, M. Ueda, T. Kishimoto, and S. Inouye, *New J. Phys.* 11, 055035 (2009).

## Formation and collisional dynamics of ultracold $\text{Rb}_2$ in the ground $X^1\Sigma_g^+$ state in an optical dipole trap

H. K. Pechkis, R. Carollo, M. Bellos, J. Banerjee, D. Rahmlow,  
E. E. Eyler, P. L. Gould, and W. C. Stwalley

*Department of Physics, University of Connecticut, Storrs, CT 06269, USA*

We present a study of the formation and collisional loss rate of ultracold ground-state  $\text{Rb}_2$  molecules in an optical dipole trap by a focused  $\text{CO}_2$  laser. Rubidium atoms are efficiently loaded from a magneto-optical trap into the dipole trap after a brief cooling and compression stage that reduces the atomic temperature significantly, to about  $30 \mu\text{K}$ , while increasing the density to as much as  $10^{12} \text{ cm}^{-3}$ . After loading atoms into the dipole trap, a photoassociation laser is introduced to form ultracold molecules. The excited ultracold molecules spontaneously decay to the  $X^1\Sigma_g^+$  ground state, which is subsequently detected by resonance-enhanced two-photon ionization using a pulsed dye laser. This detection scheme provides vibrationally resolved spectra of the molecules, which are produced mainly in high-lying vibrational levels of the ground state. We are presently investigating vibrational quenching of these molecules due to collisions with  $^{85}\text{Rb}$  atoms. With the ultracold molecules optically trapped, their decay time is measured with and without the presence of atoms in the sample. With our state-selective detection scheme, we can measure the individual loss rates of each vibrational level. This work is supported by NSF and by a MURI award administered by AFOSR.

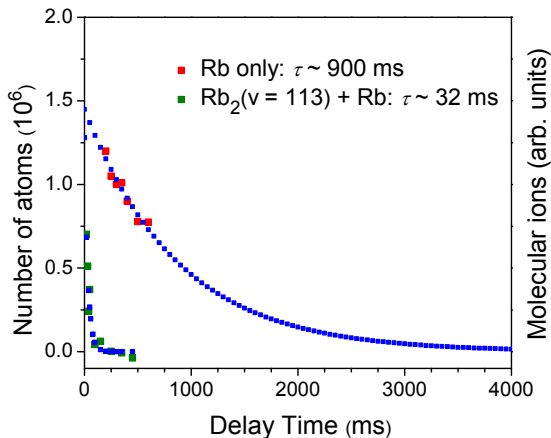


Figure 1: Preliminary results for the decay of atoms and molecules in the optical dipole trap.